IEEE Access
Multidisciplinary | Rapid Review | Open Access Journal

Received 26 February 2024, accepted 19 March 2024, date of publication 27 March 2024, date of current version 16 April 2024.

Digital Object Identifier 10.1109/ACCESS.2024.3382189

SURVEY

Applications of Zeroing Neural Networks: A Survey

TINGLEI WANG[1,2], ZHEN ZHANG[2,3], YUN HUANG[1], BOLIN LIAO[1], AND SHUAI LI[4,5], (Senior Member, IEEE)

[1]School of Computer Science and Engineering, Jishou University, Jishou 416000, China
[2]School of Communication and Electronic Engineering, Jishou University, Jishou 416000, China
[3]School of Electronic Information and Electrical Engineering, Changsha University, Changsha 410073, China
[4]Faculty of Information Technology and Electrical Engineering, University of Oulu, 90570 Oulu, Finland
[5]Technology Research Center of Finland (VTT), 90570 Oulu, Finland

Corresponding authors: Bolin Liao (bolinliao@jsu.edu.cn) and Shuai Li (shuai.li@oulu.fi)

This work was supported in part by the National Natural Science Foundation of China under Grant 62066015 and Grant 62006095.

ABSTRACT Time-varying problems are prevalent in engineering, presenting a significant challenge due to the fluctuations in parameters and goals at different time points. The zeroing neural network (ZNN), a specialized form of recurrent neural network (RNN) developed by Zhang et al., has gained attention for its rapid convergence speed and robustness making it a valuable tool for real-time solving of diverse time-varying problems. This review article explores the practical applications of ZNN across various domains in the past two decades, specifically focusing on robot manipulator path tracking, motion planning, and chaotic systems. The comprehensive scope of this review is essential for researchers and beginners looking to grasp the efficacy of ZNN in addressing practical challenges in diverse fields.

INDEX TERMS Time-varying problems, zeroing neural network (ZNN), robustness, robot manipulator.

I. INTRODUCTION

Time-varying problems are characterized by changes in their attributes and adjustments at different time points. These problems are subject to temporal influences, resulting in variations in constraints, parameters, and objectives. Addressing these problems necessitates considering the temporal factor and may require adaptively adjusting solutions to accommodate different time points. Time-varying problems are widespread in fields such as engineering, economics, and ecology [1], [2], [3], among others. However, solving these time-varying problems presents numerous challenges due to their inherent complexity and dynamic nature. The real-time generation of accurate results emerges as the primary challenge.

The rapid development of neural networks has led to their widespread application across various fields, with outstanding performance observed in addressing static problems, including computer vision [4], natural language processing [5], and speech recognition [6]. However, these networks exhibit limitations in addressing time-varying problems. To tackle this, in 2001, Zhang and colleagues officially introduced a specific type of recurrent neural network (RNN) known as the zeroing neural network (ZNN). With further research into the ZNN model, an increasing number of ZNN variant models have emerged [7], [8], [9], [10], [11], demonstrating superior performance compared to the original model. Particularly noteworthy are two key advancements: (1) Jin et al. introduced the integration-enhanced Zhang neural network (IEZNN) model in 2016 [12], showcasing robust noise resistance, and (2) Liao et al. proposed the complex noise-resistant zeroing neural network (CNRZNN) in 2022, which further enhanced the network's noise resistance, performing well against linear noise. At the same time [13], The ongoing research and the introduction of diverse nonlinear activation functions have notably enhanced the convergence speed of ZNN-related models [14], encompassing Li activation functions [7], power-sum activation functions [15], power-sigmoid activation functions [16], hyperbolic sine activation functions [17], sign-bi-power activation functions [18], NF1 and NF2 activation functions [19], FAESAF and FASSAF activation functions [20] and so

The associate editor coordinating the review of this manuscript and approving it for publication was Chao Tong.

on. Notably, ZNN's ability to employ the time derivative of time-varying parameters to effectively track solutions stands out as a crucial feature. This characteristic allows ZNN to achieve automatic equilibrium based on the principle of error reduction, drawing state values closer to the system's zero or equilibrium points. Additionally, the error function in ZNN replaces the role of gradients in gradient neural networks and does not rely on specific cost functions. Prior research has indicated ZNN's advantages in solving time-varying problems, indicating excellent stability and convergence. It is these capabilities that enable ZNN to excel in addressing time-varying problems, such as the inverse of time-varying matrix [21], [22], [23], [24], [25] and the time-varying matrix equation [26], [27], [28], [29], [30], [31], [32], [33].

Due to its exceptional performance in addressing time-varying problems, the utilization of ZNN has become widespread across various fields, including robotics [34], [35], [36], [37], chaotic systems [38], image processing [39], mathematics [40], [41], [42], [43], [44], [45], and more. Many scenarios encountered in these domains involve time-varying and dynamic problems. Specifically, in the field of robotics, tasks such as path tracking [1], [46] and motion planning [47], [48] in robotic arms represent significant examples of time-varying problems. These activities necessitate high noise immunity in the system. However, as ZNN research has progressed, the noise immunity of new ZNN models has markedly improved to meet the demands of these application scenarios effectively. Therefore, it is essential to present a comprehensive overview of ZNN applications in various fields.

The comprehensive review of the relevant ZNN models for solving time-varying problems is detailed in [49] and [50]. Based on this, the current article offers an overview and assessment of the specific applications of ZNN in addressing time-varying problems. The remaining content will be organized into four sections. Section II and Section III provide comprehensive summaries of the applications of ZNN in manipulator path tracking and manipulator motion planning, respectively. Additionally, a brief analysis of the application process will be provided. Moving on to Section IV, an in-depth review of the remarkable performance of ZNN in chaotic systems will be presented, along with a concise explanation of various chaotic systems. Section V will provide a succinct summary of the applications of ZNN in other fields, encompassing topics such as pendulum tracking of IPC systems and image processing. Lastly, Section VI will offer a comprehensive summary of the entire article, consolidating and reinforcing the key findings and contributions.

II. APPLICATION IN ROBOT MANIPULATOR PATH TRACKING

The utilization and implementation of ZNN models in robotics revolve around addressing a wide range of time-varying problems within the field. Path tracking stands out as a notable domain to apply these models.

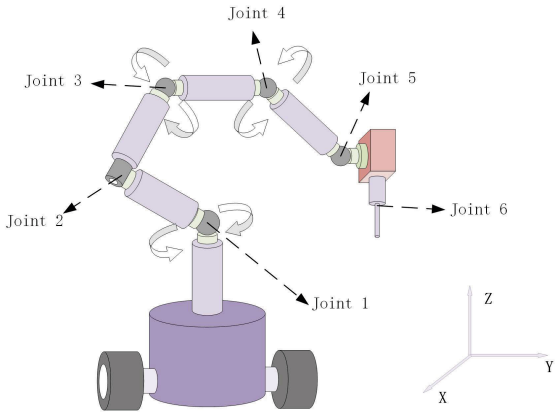

FIGURE 1. 3-D model of a mobile robot manipulator.

Robot manipulator path tracking refers to the precise tracking and execution of predefined paths or motions by a robotic arm through the utilization of computer vision and control algorithms. This technology holds significant importance in a wide range of practical applications across industries [51], [52], military organizations [53], and public services [54].

As the scope of application scenarios continues to expand, the demands for robustness and accuracy in robotic arm path tracking have become increasingly stringent. Notably, in domains such as precision manufacturing, medical surgery, and material handling, the ability to accurately track paths is pivotal in ensuring product quality, surgical precision, and efficient material handling. Consequently, the development of effective path tracking algorithms capable of handling diverse forms of interference and noise while maintaining a high level of accuracy is of utmost importance

Robot manipulators encompass various types, such as mobile manipulators [55], dual manipulators [36], redundant-manipulator [56] and so on. Despite their differences, these manipulators encounter similar challenges when it comes to path tracking, primarily revolving around the inverse kinematics problem. To illustrate the applications of ZNN in both continuous-time and discrete-time scenarios, this section will focus on mobile manipulators as a primary representative example.

A. CONTINUOUS TIME ZNN IN PATH TRACKING

The mobile manipulator represents a frequently encountered type of manipulator, featuring both a mobile platform and a fixed manipulator securely affixed to the platform (Figure 1). While the forward kinematics problem for all manipulators remains relatively straightforward and can be resolved analytically, attaining an accurate solution for the inverse kinematics problem, particularly in real-time situations, presents inherent challenges [57], [58]. In general, the forward kinematic equations for robot manipulators, at both the position level and the velocity level, can be

expressed as follows:

$$\begin{aligned} r(t) &= f(\theta(t)), \\ \dot{r}(t) &= J(\theta(t))\dot{\theta}(t), \end{aligned} \tag{1}$$

where, $\theta(t)$ and $\dot{\theta}(t)$ denote the joint position vector and the joint velocity vector, respectively. Additionally, $r(t)$ signifies the position vector of the end-effector relative to the world coordinate system, and $f(\cdot)$ denotes a smooth nonlinear mapping function, $J(\theta(t))$ is defined as $J(\theta(t)) = \partial(\theta(t))/\partial\theta$.

To address the accurate computation of time-varying inverse kinematics for mobile robots, in 2014, Xiao et al. proposed the utilization of a ZNN model [59]. They theoretically demonstrated that the ZNN model exponentially converges globally to the solution of the inverse kinematics problem for mobile manipulators.

The error function for the robotic arm path tracking can be obtained from reference [59]:

$$E(t) = r_w - r(t), \tag{2}$$

where $r_w(t)$ is desired path to be tracked.

The design equation for the original ZNN model can be obtained from reference [59]:

$$\dot{E}(t) = -\gamma E(t), \tag{3}$$

where design parameter $\gamma > 0$. By combining equations (1), (2) and (3), we can derive the ZNN model for solving the time-varying inverse kinematics problem in wheeled mobile manipulators:

$$J(\theta(t))\dot{\theta} = \dot{r}_w(t) + \gamma(r_w(t) - f(\theta(t))), \tag{4}$$

Based on the final model (4), extensive experiments were conducted to evaluate its performance. The results demonstrate that the ZNN method offers higher accuracy in solving the inverse kinematics problem of wheeled mobile manipulators compared to the conventional GNN approach. Specifically, the solution accuracy of the ZNN model is approximately 1000 times greater than that of the GNN solution when γ=1. Moreover, as the value of γ increases, the accuracy of the ZNN model solution continues to improve. This advantage of the ZNN method stems from its predictive nature, whereas the GNN method belongs to a tracking approach. The superiority of ZNN in solving such problems is evident through these findings.

Despite the notable success of ZNN models in addressing the inverse kinematics problem of manipulators, the continuous development of ZNN has led to the proposal of new models that exhibit faster convergence speed and greater noise resistance. In 2017, Xiao et al. introduced a novel ZNN model called the finite-time Zhang neural network (FTZNN), which significantly accelerated the convergence rate and was theoretically and analytically proven to achieve convergence in finite time. This advancement serves to substantially enhance the accuracy of solutions for the inverse kinematics problem in manipulators [60].

From reference [60], we can derive the design equation of FTZNN as:

$$\dot{E}(t) = -\gamma(k_1 E(t) + k_2 E^{q/p}(t)), \tag{5}$$

where the design parameters p and q represent positive odd integers satisfying $p > q$, while k_1 and k_2 are both positive values. As defined earlier, γ maintains its previous definition. In [60], it is theoretically established that this design equation offers advantages over the traditional ZNN design equation(3).

Simultaneous solution of equations (1) and (5) yields the model for solving the inverse kinematics problem in wheeled mobile manipulators using the FTZNN approach [60]:

$$\begin{aligned} J(\theta(t))\dot{\theta} = \dot{r}_w(t) &+ \beta_1(r_w(t) - f(\theta(t))) \\ &+ \beta_2(r_w(t) - f(\theta(t)))^{p/q}, \end{aligned} \tag{6}$$

where $\beta_1 = \gamma k_1 > 0$, $\beta_2 = \gamma k_2 > 0$.

In the simulation experiment conducted in [60], the tracking of an elliptic trajectory utilizing only the end-effector position was performed. Remarkably, the experiment achieved exceptional results with an error of less than $3\times10-5$ m when $\beta_1 = \beta_2 = 1$. This outcome effectively illustrates the feasibility of the model (6) and underscores the superiority of the FTZNN approach in solving the inverse kinematics problem for wheeled mobile manipulators.

Given the significant presence of noise interference in practical applications, there is an increasing demand for noise resistance during the path tracking process of manipulators [61]. To meet this demand, Chen et al. proposed the robust zeroing neural dynamics (RZND) model in 2018 [62], specifically designed to address the inverse kinematics problem in wheeled mobile manipulators. This model exhibits remarkable noise resistance capabilities, effectively countering four common types of time-varying noise. With its exceptional noise resistance, the implementation of this model significantly enhances the stability of wheeled mobile manipulators in real-world applications.

From reference [62], we can derive the design equation of RZND as:

$$\dot{E}(t) = -\gamma E(t) - \lambda \int_0^t E(\tau)\mathrm{d}\tau,$$

where design parameters $\gamma > 0$ and $\lambda > 0$

The dynamic equation of the RZND model for time-varying inverse kinematics problem of wheeled mobile manipulators as follows:

$$\begin{aligned} J(\theta(t))\dot{\theta} = \dot{r}_w(t) &+ \gamma(r_w(t) - f(\theta(t))) \\ &+ \lambda \int_0^t r_w(\tau) - f(\theta(\tau))\mathrm{d}\tau. \end{aligned} \tag{7}$$

The block diagram of the RZND model (7), which addresses the tracking control problem of mobile robot manipulators under the influence of external disturbances, is depicted in Figure 2.

Based on the simulation results reported in [62], the position error of the end-effector during path tracking tasks

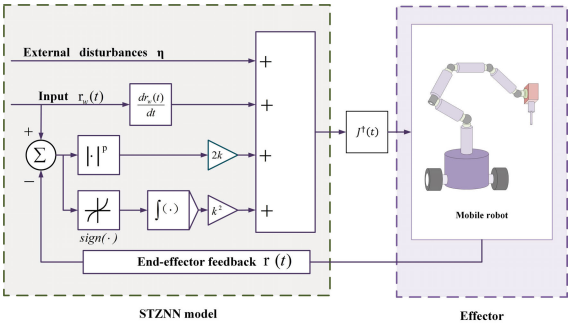

FIGURE 2. Block diagram represents the STZNN model integrating external disturbances to address the tracking control problem of mobile robot manipulators. In this context, $J^{\dagger}(t)$ signifies the pre-multiplication operators by the pseudoinverse matrix $J^{\dagger}(t)$.

converges to 0 when subjected to linear noise, sinusoidal noise, exponential decay noise, and continuous bounded random noise. This observation confirms the outstanding inherent anti-interference performance of the proposed RZND model (7), making it well-suited for path tracking applications in wheeled mobile manipulators that experience time-varying disturbances.

In the previously mentioned utilization of the FTZNN(6) and RZND(7) models for solving the inverse kinematics problem in mobile manipulators, improvements were introduced to the original ZNN model in two pivotal areas: finite-time convergence and noise immunity. As the application scenarios of manipulators continue to advance, enhancing the convergence performance and robustness of the inverse kinematics problem in manipulators has become a significant research focus. In line with this objective, in 2020, Chen et al. proposed the STZNN model, which leverages the supertwisting (ST) algorithm for tracking control in mobile robots [63]. Remarkably, this model facilitates rapid and robust control processes, effectively meeting the practical application requirements of mobile manipulators. From reference [63], we can derive the design equation of STZNN as:

$$\dot{E}(t) = -2k\psi^{p}E(t) - k^{2}\int_{0}^{t}\text{sign}(E(\tau))\text{d}\tau,$$

with the i th element of vector mapping $\psi^{p}(\cdot)$ depicted in:

$$\psi_{i}^{p}(E_{i}(t)) = \begin{cases} |E_{i}(t)|^{p}, & E_{i}(t) > 0, \\ 0, & E_{i}(t) = 0, \\ -|E_{i}(t)|^{p}, & E_{i}(t) < 0, \end{cases}$$

where k is the design parameters. In addition, $p = 1/2$ is set.

The dynamic model applied to the mobile manipulator is depicted below and the block diagram shown in Figure 2 clearly presents the main principle of the control strategy:

$$J(\theta(t))\dot{\theta} = \dot{r}_{w}(t) + 2k\psi^{p}(r_{w}(t) - f(\theta(t))) + k^{2}\int_{0}^{t} sign(r_{w}(\tau) - f(\theta(\tau)))\text{d}\tau. \quad (8)$$

Chen and colleagues [63] conducted a comparison between the CZNN model [64] and existing models, showing that the CZNN model demonstrates exponential convergence in undisturbed conditions but may experience steady-state errors in the presence of disturbances. They highlighted the limitations of current models, such as indefinite prolongation of convergence time and relatively insufficient analysis of stability and asymptotic convergence, underscoring the significance of convergence performance and robustness in complex environments. Subsequently, they presented the design process of the STZNN model and its innovative approach in simultaneously improving convergence time characteristics and robustness when addressing the path tracking issue in mobile robot manipulators. The STZNN model was also emphasized for its thorough theoretical analysis, showing global stability, finite-time convergence capability, and robustness.

In the applications of M-shaped path-tracking and Lissajous-shaped path-tracking, extensive testing and comparison with the CZNN model confirmed the effectiveness and practical potential of the STZNN model in addressing the path tracking issue for mobile robot manipulators. The STZNN model demonstrated significant advantages in path tracking control, especially in terms of convergence performance and robustness, surpassing conventional models like the CZNN model.

This innovative theoretical analysis and practical testing provide robust support and evidence for the application of the STZNN model in addressing the path tracking issue of mobile robot manipulators.

With the continuous advancements in ZNN models, an increasing number of models have emerged to address the inverse kinematics problem in wheeled mobile manipulators, leading to the maturation of path tracking applications in these manipulators. For instance, in 2020, Jin et al. introduced an interference-tolerant fast convergence zeroing neural network (ITFCZNN) that employs a novel activation function (NAF) [65]. Through experimental verification, the applicability and feasibility of ITFCZNN in path tracking for wheeled manipulators under interference and noise conditions were substantiated. In 2021, Chen et al. proposed a unified framework of ZNN that incorporated a novel neural-network-based model [66]. By leveraging the Lagrange method, this model converted the time-dependent nonlinear optimization problem, which includes multiple types of constraints, into a time-dependent equality system. Termed the multi-constrained ZNN (MZNN), this model inherently exhibits the effectiveness of exponential convergence by utilizing time-derivative information. Through nonlinear optimization control applications in mobile robots, it was convincingly demonstrated that MZNN possesses the physical validity required for controlling mobile robots with performance index optimization and multiple physical limit constraints. In 2022, Luo et al. proposed a new hyperbolic tangent varying-parameter ZNNs (HTVP-ZNNs) with time-varying DCPs (designed convergence parameters) and a robust HTVP-ZNNs (HTVPR-ZNNs) [67], which exhibited excellent performance in trajectory tracking tasks

of the robot. In 2023, Lan et al. devised a non-linear activation function and leveraged it to propose a non-linearly activated ZNN (NAZNN) model [68]. The application of this NAZNN model in addressing the trajectory tracking fault problem of a manipulator effectively yielded positive results, as demonstrated through experimental analysis.

B. DISCRETE TIME ZNN IN PATH TRACKING

Previous studies have shown that continuous time ZNN models are highly effective in the field of manipulator path tracking. However, the direct implementation of continuous time ZNN models on digital computers poses challenges due to the need for a stable sampling interval (τ) throughout the computation process [69], [70]. Moreover, continuous-time ZNN models assume instantaneous communication and response among neurons, but this is not feasible in digital circuits due to inherent sampling gaps and unavoidable time delays.Consequently, researchers have developed discrete ZNN models that have yielded favorable results in the domain of manipulator path tracking.

In order to improve the applicability of the discrete-time ZNN model in manipulator path tracking, in 2014 Jin and colleagues first proposed and investigated a Taylor-type numerical differentiation formula. Subsequently, they introduced the T-ZNN-K model and T-ZNN-U model [71], which were shown to have a residual error of $O(\tau 3)$. This model exhibited outstanding performance in manipulator path tracking.

From reference [71], we can derive the design equation of T-ZNN-U as:

$$\begin{aligned} X_{k+1} = &-X_k(\frac{11}{6}A_k - 3A_{k-1} + \frac{3}{2}A_{k-2} - \frac{1}{3}A_{k-3})X_k \\ &- h(X_kA_kX_k - X_k) + \frac{3}{2}X_k - X_{k-1} + \frac{1}{2}X_{k-2}, \quad (9) \end{aligned}$$

where step-size $h = \tau\gamma > 0$.In the context of the inverse kinematics problem in robotic arms,the analytical solution to the inverse-kinematic problem is equation(1), where $J^{\dagger}(\theta(t))$ is the pseudoinverse of time-varying Jacobian matrix. We need to obtain $J^{\dagger}(\theta(t))$ in real time t for the control of the robot. Defining $A_k = J(\theta(k\tau))$ and exploit the aforementioned ZNN models (9) to solve $J^{\dagger}(\theta(t))$.

In the experiment, Jin et al. found that the discrete ZNN model, generated using Newton's iteration method for path tracking of a five-link planar robot manipulator, produced a maximum position error approximately 10 times larger than that of the T-ZNN-U model [71]. Additionally, in 2016, Liao et al. compared the position error generated by the T-ZNN-U model with that of the discrete ZNN model, which was created using Euler's method for manipulator path tracking. The results indicated that the T-ZNN-U model exhibited the smallest error [72], thereby further highlighting the superiority of the T-ZNN-U model proposed by Jin et al. in the application of manipulator tracking.

Sun et al. aimed to enhance the accuracy of manipulator path tracking. They introduced a high accuracy first-order derivative approximation formula for discretization, and subsequently developed two models: HADTZTM-K (high accuracy discrete-time zeroing-type model with known derivative information) and HADTZTM-U (high accuracy discrete-time zeroing-type model with unknown derivative information) [73]. These models were applied to the path-tracking of a four-link planar manipulator, yielding favorable outcomes.

From reference [73], we can derive the design equation of HADTZTM-K as:

$$\begin{aligned} X_{k+1} = &\frac{5}{24}X_k + \frac{1}{2}X_{k-1} + \frac{1}{4}X_{k-2} + \frac{1}{6}X_{k-3} - \frac{1}{8}X_{k-4} \\ &+ 2A_k^{+}(\tau\dot{B}_k - \tau\dot{A}_kX_k - h(A_kX_k - B_k)), \quad (10) \end{aligned}$$

And the HADTZTM-U is:

$$\begin{aligned} X_{k+1} = &\frac{5}{24}X_k + \frac{1}{2}X_{k-1} + \frac{1}{4}X_{k-2} + \frac{1}{6}X_{k-3} \\ &- \frac{1}{8}X_{k-4} + 2A_k^{+}(\frac{25}{12}B_k - 4B_{k-1} + 3B_{k-2} \\ &- \frac{4}{3}B_{k-3} + \frac{1}{4}B_{k-4} - (\frac{25}{12}A_k - 4A_{k-1} \\ &+ 3A_{k-2} - \frac{4}{3}A_{k-3} + \frac{1}{4}A_{k-4})X_k \\ &- h(A_kX_k - B_k)), \quad (11) \end{aligned}$$

where step size $h = \gamma\tau > 0$, and τ denotes the sampling gap. It is worth noting that the path-tracking problem of a planar manipulator bears resemblance to that of wheeled mobile manipulators, with both being amenable to formulation using formula (4), so the $A_{k+1} = J(\theta(t_{k+1}))$ and $B_{k+1} = \dot{r}_w(t_{k+1}) + \gamma(r_w(t_{k+1}) - f(\theta(t_{k+1})))$.

In [73], the authors utilized the proposed HADTZTM-K (10) and HADTZTM-U (11) models to enable three-leaf-clover path tracking for a four-link planar manipulator. Initially, the superior performance of the proposed HADTZTM-K model was validated under various parameter h settings through numerical simulations. When compared to DTZTM and DTETM, the HADTZTM-K model exhibited reduced positional error, with the maximum positional error being approximately 2.87 times smaller than that of DTZTM. Furthermore, it was observed that the positional error of the DTZTM model decreased with increasing parameter h, though the minimum positional error remained approximately 1.2-1.3 times larger than that of HADTZTM-K. Finally, the effectiveness of HADTZTM-K in path tracking was confirmed through additional numerical simulations, illustrating its ability to achieve minimal positional error.

The application of discrete-time ZNN models in path-tracking problems has become increasingly significant with rapid development. In 2021, Liu et al. introduced a novel Taylor-type difference rule with an error pattern of $o(\tau^4)$, and subsequently proposed the FDNTZNN model (a high accuracy noise-tolerant five-step discrete-time zeroing neural network) [74]. This model exhibited exceptional accuracy in manipulator path tracking.

From the [74], we can infer that the FD-NTZNN-k model is:

$$\begin{cases} X_{k+1} = 2A_k^{-1}(-\tau(\frac{25}{12}A_k - 4A_{k-1} + 3A_{k-2} - \frac{4}{3}A_{k-3} \\ \quad +\frac{1}{4}A_{k-4})X_k - h(A_kX_k - I) - h_1J_k) + 2\tau\eta_k \\ \quad +\frac{5}{24}X_k + \frac{1}{2}X_{k-1} + \frac{1}{4}X_{k-2}) + \frac{1}{6}X_{k-3} - \frac{1}{8}X_{k-4}, \\ J_{k+1} = 2\tau(A_kX_k - I) + \frac{5}{24}J_k + \frac{1}{2}J_{k-1} + \frac{1}{4}J_{k-2} \\ \quad +\frac{1}{6}J_{k-3} - \frac{1}{8}J_{k-4}, \end{cases}$$

where τ is sampling time, $h = \tau\gamma > 0$ signifies the step size, $h_1 = \tau\lambda > 0$, η is unknown noises and similar to formula (9) $A_k = J(\theta(k\tau))$.

In [74], Jin et al. employed the FDNTZNN model in the path tracking of a two-link planar manipulator. They conducted a comparative analysis between the FDNTZNN model and the EDNTZNN model (euler-type discrete-time noise-tolerant), considering error in different noise scenarios ranging from no noise to constant, linear, and random noise. The FDNTZNN model exhibited the lowest maximal steady-state residual errors, indicating the superiority of FDZNN in its application to manipulator path tracking.

In 2023, Wu and colleagues integrated the ZND (zeroing neural dynamics) model with the GND (gradient neural dynamics) model to develop the CGZND (continuous gradient-zeroing neural dynamics) model. Subsequently, they developed the order-6 discrete gradient-zeroing neural dynamics (O6-DGZND) algorithm, aiming for easy implementation in computer systems and digital hardware. The algorithm was designed by simultaneously combining the order-6 Zhang time discretization (O6-ZTD) formula and the order-6 extrapolation (O6-E) formula [75]. This algorithm was successfully employed to track the movement of a UR10 manipulator

From the [75], we can obtain that the O6-DGZND model is:

$$\begin{cases} Z_0 = Z(0), \\ Z_{k+1} = -\frac{h}{b_0}(Z_kA_kA_k^{\mathrm{H}} - I)A_kA_k^{\mathrm{H}} - \frac{\tau}{b_0}Z_k(\dot{A}_kA_k^{\mathrm{H}} \\ \quad +A_k\dot{A}_k^{\mathrm{H}})Z_k - \frac{1}{b_0}\sum_{i=1}^{9} b_iZ_{k+1-i} \\ \tilde{A}_{k+1}^{H} = 6A_k^{\mathrm{H}} - 15A_{k-1}^{\mathrm{H}} + 20A_{k-2}^{\mathrm{H}} - 15A_{k-3}^{\mathrm{H}} + 6A_{k-4}^{\mathrm{H}} \\ \quad -A_{k-5}^{\mathrm{H}}, \\ X_{k+1} = \tilde{A}_{k+1}^{\mathrm{H}}Z_{k+1}, \end{cases} \tag{12}$$

where $Z_k = (A_kA_k^H)^{-1}$,the coefficients b_i with $i = 0, 1, \ldots, 9$ are set as the first row of Table 1 in [76], $h = \tau\gamma$ denotes the step length, $\tilde{A}_{k+1}^H$ is the approximation of matrix A_{k+1}^H and similar to formula (9) $A_k = J(\theta(k\tau))$.

The O6-DGZND algorithm demonstrates exceptional accuracy in the task of manipulator tracking. This high accuracy is primarily attributed to the truncation error of the O6-DGZND algorithm (12), which is $o(\tau^6)$. The introduction of the O6-DGZND algorithm represents a significant advancement in the utilization of ZNN for manipulator path tracking

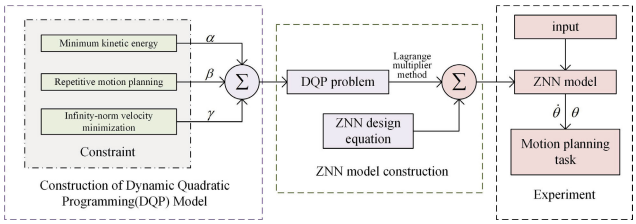

FIGURE 3. Overall framework for the manipulator motion planning.

III. APPLICATION IN ROBOT MANIPULATOR MOTION PLANNING

Robotic manipulators have become increasingly prevalent in various applications, excelling not only in completing path tracking tasks but also in performing motion planning functions [77], [78], [79], [80], [81], [82]. Motion planning involves the formulation of a robot's motion path and action sequence, entailing movement and operation in complex environments while considering multiple constraints and goals to ensure the safe and efficient completion of tasks. This demands advanced real-time data processing capabilities. ZNN demonstrates exceptional proficiency in addressing time-varying problems, empowering robots to dynamically integrate environmental changes and time-varying constraints for optimal action planning. This adaptability becomes crucial in complex robotic tasks, demanding agile decision-making and efficient resource allocation. Redundant robot manipulators play a crucial role in motion planning tasks due to their higher degrees of freedom (DOF) compared to the workspace, rendering them relatively flexible [56]. In the case of an end-effector tracking task, redundant robot manipulators offer numerous solutions, but additional constraints, including repetitive motion control, obstacle avoidance, and manipulability optimization, can effectively limit their movement [83]. With these constraints, motion planning for redundant robot manipulators can be effectively realized using ZNN models, ensuring precise task execution(refer to Figure 3).

In 2016, Jin et al. introduced the modified zhang neural network (MZNN) model to address time-varying quadratic programming problems. Their experimental findings demonstrated that the utilization of MZNN effectively resolves the joint-drift phenomenon in robot manipulator path tracking tasks when dealing with measurement noise [84]. Subsequently, in 2017, Jin et al. proposed and investigated a parallel minimization method for fault-tolerant motion planning of redundant manipulators at various levels [37]. This approach incorporates physical constraints in joint space while accounting for robot kinematics and dynamics. The method transforms into a quadratic programming

problem with equality constraints and is resolved utilizing a discrete-time recurrent neural network. Finally, simulation experiments were conducted on a six-bar planar redundant robot to validate the viability of the approach.

The physically-constrained redundant robot manipulators can be formulated into the following standard QP in terms of joint-acceleration level can be obtained from [37]:

$$\begin{aligned} \text{minimize} \quad & \alpha(\ddot{\theta}^{\mathrm{T}} W \ddot{\theta}/2 + p^{\mathrm{T}}\ddot{\theta}) + \beta\tau^{\mathrm{T}}\tau/2 \\ \text{subject to} \quad & J(\theta)\ddot{\theta} = b, \\ & \eta^{-} \le \ddot{\theta} \le \eta^{+}, \end{aligned} \tag{13}$$

where $\alpha \in (0,1)$ and $\beta \in (0,1)$ are the weighting factors with $\alpha + \beta = 1$, $W = I$, $p = (\mu + \nu\dot{\theta}) + \mu\nu(\theta - \theta(0))$ with $\mu > 0$ and $\nu > 0$, $\tau = H\ddot{\theta} + c_\tau(\dot{\theta}, \theta) + g_\tau(\theta)$, $b = \ddot{r_a} + K_v(\dot{r_d} - J(\theta)\dot{\theta}) + K_p(r_d - f(\theta))$ and η^- and η^+ are the new bound constraint of joint acceleration [85], [86].

In addition, K_p and K_v are positive-definite symmetric gain matrices for position-error and velocity-error feedbacks, H denotes the inertia matrix, c_τ denotes the Coriolis/centrifugal force vector and g_τ denotes the gravitational force vector.

And from [37] we can get the discrete-time recurrent neural networkfor solving online the QP problem.

$$u^{k+1} = u^k - \frac{\|e(u^k)\|_2^2}{\|(M^{\mathrm{T}} + I)e(u^k)\|_2^2}(M^{\mathrm{T}} + I)e(u^k), \tag{14}$$

the specific symbol meanings in equation (14) are explained in detail in the reference [37].

The author in [37] conducted motion planning for square path tracking by constraining the motion of a six-link planar redundant robot, employing an enhanced ZNN model for iterative computation, yielding favorable outcomes. During the simulation experiment, the six-link planar redundant robot adeptly accomplished the task even with the first five joints being faulty from on $t = 15s$, indisputably showcasing the ZNN model's superiority in robot manipulator motion planning.

In 2018, Zhang et al. introduced a new varying-parameter convergent-differential neural network (VP-CDNN) derived from ZNN, effectively resolving the issues of joint-angular-drift in redundant robot manipulators. This model was applied using a six-degree-of-freedom (DOF) Kinova Jaco^2 robot [87].

The feedback considered joint-angular-drift-free (FC-JADF) scheme of a redundant robot manipulator [87] is expressed as follows:

$$\begin{aligned} \text{minimize} \quad & \dot{\theta}^{\mathrm{T}} W \dot{\theta}/2 + c^{\mathrm{T}}\dot{\theta} \\ \text{subject to} \quad & J(\theta)\dot{\theta} = b, \end{aligned}$$

where the definition of $\dot{\theta}$ and $J(\theta)$ are similar to equation(1), $W = \|\theta(t) - \theta(0)\|_2^2$ and $b = \dot{r} + K(r - f(\theta))$,K is a positive-definite symmetric feedback-gain matrix.

The implicit-dynamic equation for the redundant robot manipulator [87] is as follows:

$$A(t)\dot{y}(t) = -\dot{A}(t)y(t) - (\gamma + t^{\gamma})\Phi(A(t)y(t) - g(t)) + \dot{g}(t),$$

where

$$A(t) = \begin{bmatrix} W(t) & J^{\mathrm{T}}(\theta(t)) \\ J(\theta(t)) & 0 \end{bmatrix},$$
$$y(t) = \begin{bmatrix} \dot{\theta}(t) \\ \lambda(t) \end{bmatrix}, g(t) = \begin{bmatrix} -c(t) \\ b(t) \end{bmatrix},$$

In addition, $\lambda(t)$ is a vector of Lagrange multiplier, $\gamma > 0$ is a scalar-valued parameter.

Through the execution of starfish-path tracking and cardioid-path tracking tasks on a six-degree-of-freedom (DOF) Kinova Jaco^2 robot [87], and subsequent comparison of the outcomes between joint-angular-drift and joint-angular-drift-free scenarios, it can be inferred that VP-CDNN effectively mitigates the joint-angular-drift issue in redundant robot manipulators.

In 2021, Yang et al. introduced a concise continuous ZNN (CZNN) which was subsequently discretized using two discrete formulas to yield two concise discrete ZNN (DZNN) controllers [88]. These controllers were then applied to the end-effector tracking task involving obstacle avoidance for redundant manipulators. The findings demonstrated the effectiveness of DZNN in motion planning for obstacle avoidance.

From reference [88] we can obtain the obstacle avoidance formulation at velocity level:

$$\begin{aligned} 2(p_{c,i}(t) - p_o(t))^{\mathrm{T}} J_{c,i}(\theta(t))\dot{\theta}(t) - 2\varphi_i(t)\dot{\varphi}_i(t) = \\ - \gamma((p_{c,i}(t) - p_o(t))^{\mathrm{T}}(p_{c,i}(t) - p_o(t)) - d_i^2 - \varphi_i^2(t)) \\ + 2(p_{c,i}(t) - p_o(t))^{\mathrm{T}}\dot{p}_o(t), \end{aligned}$$

where p_o is position of obstacle, $p_{c,i}$ is position of the ith critical point, $J_{c,i}(\theta(t)) = \partial_{c,i}(t)/\partial\theta(t)$ denotes the Jacobian matrix for the critical point in the ith link, d_i is safe distance between obstacle and the ith link, φ_i is additional variable, γ is ZNN design parameter.

From reference [88], we can derive the second-order DZNN (SDZNN)(15) and the third-order DZNN (TDZNN)(16) as:

$$\omega_{k+1} = \omega_k + \tau\dot{\omega}_k, \tag{15}$$

$$\omega_{k+1} = \omega_k + \frac{3\tau}{2}\dot{\omega}_k - \frac{\tau}{2}\dot{\omega}_{k-1}, \tag{16}$$

where τ being the sampling gap.

The six-degree-of-freedom UR5 manipulator was employed to trace the end effector along a three-ring path under the control of equation(15) and equation(16). The evaluation encompassed static, vertically moving, and 3-D moving obstacles. The application of the SDZNN and TDZNN controllers for manipulator control notably averted collisions with the obstacles, in contrast to the traditional SDPI controller, which resulted in collisions [88]. These findings distinctly underscore the superior efficacy of the ZNN model in resolving issues related to manipulator motion planning.

In 2021, Yang et al. introduced a 6-step discretization formula and a 4-step backward difference formula to create a 6-step DZNN (6SDZNN) model [89]. When

compared to the standard discrete zeroing neural network (DZNN) model, the 6SDZNN model demonstrates improved accuracy and enhanced capability in addressing the issue of repetitive motion control in redundant manipulators.

From reference [89] the repetitive motion control scheme is described as:

$$\begin{aligned} &\text{minimize} \quad \dot{\theta}^{\mathrm{T}}\dot{\theta}/2 + \lambda(\theta(t) - \theta(0))^{\mathrm{T}}\dot{\theta}(t) \\ &\text{subject to} \quad J(\theta)\dot{\theta} = \dot{r}_w - \lambda(r(t) - r_w(t)), \end{aligned}$$

where the symbols in question have the same definitions as those in equation(1) and equation(13).

And the 6SDZNN model is:

$$\begin{aligned} X_{k+1} = &-\frac{58}{93}X_k + \frac{71}{62}X_{k-1} + \frac{29}{31}X_{k-2} \\ &- \frac{32}{93}X_{k-3} - \frac{7}{31}X_{k-4} + \frac{7}{62}X_{k-5} \\ &- \frac{82}{31}A_k^{-1}(\hat{A}_k X_k + \hat{b}_k + hA_k X_k + hb_k), \end{aligned} \tag{17}$$

where the specific symbol meanings in equation(17) are explained in detail in the reference [89].

A physical experiment was conducted in the literature [89] to showcase the effectiveness of the 6SDZNN model(17) in addressing repetitive motion control issues. The experiment involved utilizing the Kinova Jaco^2 manipulator to execute repetitive trajectory tracking similar to lung-like path movements. Notably, the experimental outcomes revealed minimal error in the images obtained after employing the 6SDZNN for three cycles of trajectory tracking, whereas substantial errors were evident in the images generated using other models. These findings distinctly underscore the superior capability of the ZNN model in resolving repetitive motion control problems.

In 2022, Qiu et al. proposed a groundbreaking velocity layer weighted multicriteria optimization (VLWMCO) scheme, showcasing its superiority over conventional methods for robotic manipulators dealing with multiple constraints [80]. Subsequently, the VLWMCO scheme was reformulated as a dynamic quadratic programming problem and then solved using a novel DZNN model and the precision-based six-step extrapolated-backward discretization (6SEBD) rule. Its efficacy was validated through the end-effector tracking of the eight-petal flower path employing the six-degree-of-freedom Kinova Jaco^2 manipulator.

From the [80] VLWMCO scheme can be mathematically formulated as:

$$\begin{aligned} &\text{minimize} \quad \phi(\dot{\theta}(t), \theta(t), t) \\ &\text{subject to} \quad J(\theta)\dot{\theta} = s(t) \\ &\qquad\qquad \theta^- \leqslant \theta(t) \leqslant \theta^+ \\ &\qquad\qquad \theta^- \leqslant \dot{\theta}(t) \leqslant \theta^+, \end{aligned} \tag{18}$$

where the specific symbol meanings in equation(18) are explained in detail in the reference [80].

Conventional robot manipulator motion control schemes typically accommodate single or dual optimization requirements [78], [90], [91], [92]. In contrast, the VLWMCO scheme proposed by Qiu et al. can fulfill multiple optimization needs, such as minimum kinetic energy, repetitive motion planning, and infinity-norm velocity minimization. This effectively attends to the pertinent demands for robot manipulator motion planning in practical applications.

And the novel 6SEBD-based DZNN model with a truncation error of $o(\tau^7)$ is obtained as:

$$\begin{aligned} X_{k+1} = &\frac{360}{147}X_k - \frac{150}{49}X_{k-1} + \frac{400}{147}X_{k-2} - \frac{75}{49}X_{k-3} \\ &+ \frac{72}{147}X_{k-4} - \frac{10}{147}X_{k-5} + \frac{20\tau}{49}(6\dot{X}_k - 15\dot{X}_{k-1} \\ &+ 20\dot{X}_{k-2} - 15\dot{X}_{k-3} + 6\dot{X}_{k-4} - \dot{X}_{k-5}). \end{aligned} \tag{19}$$

In the literature [80], the performance of using the conventional INVM scheme and the resultant DZNN model, compared with using the VLWMCO scheme and the 6SEBD-based DZNN model, for end-effector tracking of the eight-petal flower path was experimentally compared. The results showed that using the conventional Infinity-norm velocity minimization scheme resulted in the actual trajectory of the end effector gradually deviating from the expected path during task execution, and undesirable joint angle drift occurred. Using the VLWMCO scheme effectively eliminated the undesirable joint angle drift, final joint velocity non-zero, and joint velocity discontinuity, which fully demonstrates the effectiveness of ZNN in solving robot manipulator motion planning.

In 2022, Tan et al. introduced a closed-loop control system based on the damping zeroing neural network (DampZNN) to achieve unified kinematic control for both redundant robots and continuum robots with unknown kinematics. This control system comprises two DampZNNs, utilized for estimating the unknown kinematic model and solving the inverse kinematics problem, respectively [93]. Subsequently, experiments were carried out on diverse platforms and robots to validate its efficacy.

The kinematic equation of a robot manipulator can be inferred from equation(1), and rom the [93] we can get DampZNN:

$$\dot{\theta}(t) = \tilde{J}_{dp}^{-1}(t)(\dot{r}_w(t) + \gamma\,\Xi(r_w(t) - r(t))),$$

where $\tilde{J}_{dp}^{-1}(t)$ is the inverse solution including damping factor λ, $\Xi(\cdot)$ is the element-wise activation function array.

Tan et al. performed three sets of experiments to confirm the superior performance of DampZNN, conducting tests on the redundant robot in V-REP, KINOVA JACO Gen2 Robot, and continuum robot. The results indicated that when a human operator guided the HIP along a specific path, the robot's bell-shaped effector followed the same trajectory with minor error, unequivocally establishing the effectiveness of DampZNN in teleoperation systems for both redundant and continuum robots.

Qiu et al. introduced a fuzzy-enhanced robust discretized zeroing neural network (FER-DZNN) model designed to address future multiconstrained nonlinear optimization (FMCNO) problems [94]. They applied this model to the motion planning of the UR5 manipulator, yielding outstanding results and showcasing the superiority of ZNN-related models in solving motion planning problems for manipulators.

The future multi-constrained nonlinear optimization (FMCNO) problem is described as below:

$$\begin{aligned} &\text{minimize} && \psi(xk+1, t_{k+1}) \\ &\text{subject to} && Q_{k+1}x_{k+1} = q_{k+1} \\ &&& R_{k+1}x_{k+1} \leqslant r_{k+1} \\ &&& d_{k+1} \leqslant x_{k+1} \leqslant p_{k+1}. \end{aligned} \tag{20}$$

The motion control problem of the UR5 manipulator with multiple constraints can be considered as a specific instance of the FMCNO problem (20). In this formulation, the objective function, coefficient matrices, and vectors of constraints are provided as follows [94]:

$$\begin{aligned} \psi(x_k, t_k) &= \frac{1}{2}x_k^{\mathrm{T}}x_k + \bar{\varsigma}(\theta_k - \theta_0)^{\mathrm{T}}x_k, \\ Q_k &= J(\theta_k), \quad q_k = \dot{z}_{d,k} + \tilde{\varsigma}(z_{d,k} - z_k), \\ R_k &= \begin{bmatrix} \ell_{1x6} \\ -\ell_{1x6} \end{bmatrix}, \quad r_k = \begin{bmatrix} \Xi k^+ \\ -\Xi k^- \end{bmatrix}, \\ d_k &= \dot{\theta}^- - \dot{\theta}^- \odot \exp(\hat{\varsigma}(\theta_k - \theta^-) \oslash (\check{\varsigma}\theta^-)), \\ p_k &= \dot{\theta}^+ - \dot{\theta}^+ \odot \exp(\hat{\varsigma}(\theta_k - \theta^+) \oslash (\check{\varsigma}\theta^+)), \end{aligned}$$

where the definition of $\dot{\theta}$ and $J(\theta)$ are similar to equation(1), $z_{d,k}$ is the end-effector desired path, $\dot{z}_{d,k}$ is the end-effector position vector, $\bar{\varsigma}$, $\tilde{\varsigma}$, $\hat{\varsigma}$, $\check{\varsigma}$ are four positive parameters, $\theta^{\pm}$ and $\theta^{\pm}$ denote the upper and lower bounds of θ_k and $\dot{\theta}_k$, respectively, $\Xi k^{\pm}$ denote the upper and lower bounds of the sum of the six joint velocities.

The FER-CZNN model is described as below:

$$\begin{aligned} u_{k+1} = u_k &- \frac{1}{2}u_{k-1} + \frac{1}{2}u_{k-2} + \frac{1261}{480}\zeta\dot{u}_k - \frac{289}{80}\zeta\dot{u}_{k-1} \\ &+ \frac{79}{20}\zeta\dot{u}_{k-2} - \frac{437}{240}\zeta\dot{u}_{k-3} + \frac{57}{160}\zeta\dot{u}_{k-4}. \end{aligned} \tag{21}$$

Based on the comparative analysis [94], it can be concluded that the FER-DZNN model exceeds the traditional ITR-DZNN model (without considering the fuzzy factor w) in addressing the motion control challenges encountered by the UR5 robotic arm under multiple constraints. The motion control problem of the UR5 manipulator with multiple constraints can be categorized as the FMCNO problem. The FER-DZNN model demonstrates exceptional performance in achieving the motion control task of the UR5 robotic arm, even in the presence of Gaussian white noise disturbances. This effectively highlights the remarkable capabilities of ZNN in robotic arm motion planning.

IV. APPLICATION IN CHAOTIC SYSTEM

Chaotic systems represent a prevalent type of nonlinear system first identified by Edward Lorenz half a century ago [95]. Since its discovery, chaotic systems have been the subject of extensive research and have found widespread application across diverse fields, such as power systems [96], financial systems [97], ecosystems [98], and secure communication [99], [100], [101]. Nevertheless, owing to their inherent traits of uncertainty, irreproducibility, and unpredictability, addressing issues related to chaotic systems has proven to be challenging. The introduction of the ZNN model has contributed to the effective resolution of problems associated with chaotic systems.

In 2023, Sondess B. Aoun et al. introduced a new noise-resistant ZNN model to address the quaternion dynamic Sylvester equation and showcased its exceptional performance in a specific application for controlling the sine function memristor (SFM) chaotic system [102].

From [102] and [103] we can obtain the SFM chaotic system:

$$\begin{cases} \dot{x}_1(t) = s(x_2(t)), \\ \dot{x}_2(t) = -\frac{1}{3}s(x_1(t)) + \frac{1}{2}s(x_2(t)) - \frac{1}{2}\eta^2 s(x_2(t))s^2(x_3(t)), \\ \dot{x}_3(t) = -s(x_2(t)) - 0.6s(x_3(t)) + \eta s(x_2(t))s(x_3(t)), \end{cases} \tag{22}$$

where $X(t) = [x1(t), x_2(t), x_3(t)]^T$ are state variables.

When taking into account uncertainties, noise, and the controller, Equation (22) can be rephrased as follows:

$$\begin{cases} \dot{x}_1(t) = s(x_2(t)) + \Delta f_1(x) + h_1(t) + u_1(t), \\ \dot{x}_2(t) = -\frac{1}{3}s(x_1(t)) + \frac{1}{2}s(x_2(t)) - \frac{1}{2}\eta^2 s(x_2(t))s^2(x_3(t)) \\ \qquad +\Delta f_2(x) + h_2(t) + u_2(t), \\ \dot{x}_3(t) = -s(x_2(t)) - 0.6s(x_3(t)) + \eta s(x_2(t))s(x_3(t)) \\ \qquad +\Delta f_3(x) + h_3(t) + u_3(t), \end{cases} \tag{23}$$

where $\Delta f_1(x)$, $\Delta f_2(x)$ and $\Delta f_3(x)$ are uncertainties of the system, $h_1(t)$, $h_2(t)$ and $h_3(t)$ refer to external disturbances, $u_1(t)$, $u_2(t)$ and $u_3(t)$ represent the controllers.

The error function for the SFM chaotic system can be obtained from [102]:

$$E(t) = X(t), \tag{24}$$

where$X(t) = [x_1(t), x_2(t), x_3(t), \ldots, x_n(t)]^T$ is the state vector of response chaotic system

From [102], the NZNN design formula can be described as:

$$\dot{E}(t) = -\lambda E(t) - \zeta \int_0^t E(\tau)\mathrm{d}\tau,$$

and the ordinary ZNN(OZNN)design formula can be described as:

$$\dot{E}(t) = -\lambda E(t),$$

combining the above two formulas with formula (23) and formula (24),controller of SFM chaotic system is:

$$U(t) = \dot{E}(t) - F(X(t)), \tag{25}$$

where $F(\cdot)$ is the nonlinear mapping vector function and $\dot{X}(t) = F(X(t))$

A comparative study was performed in [102] to assess the control of the SFM chaotic system using no ZNN controller, an OZNN controller, and an NZNN controller. The findings revealed that the SFM chaotic system, when controlled without a ZNN controller and with an OZNN controller, failed to converge to the zero point in three-dimensional space. In contrast, with the NZNN controller, both states and phases could stabilize to zero simultaneously. These experimental results fully underscore the exceptional performance and superiority of the NZNN controller in regulating the SFM chaotic system.

In 2023, Hua et al. introduced a novel complex ZNN model, DISZNN, featuring a dual integral structure designed to inherently mitigate linear noise [104]. This model was successfully utilized for controlling chaotic systems, delivering promising outcomes.

In [104], Hua applied the DISZNN model to the control of permanent magnet synchronous motor (PMSM) Chaotic System with Uncertainties and External Disturbance, and we can know that the controllable PMSM model with external disturbance and uncertainties can be constructed as:

$$\begin{cases} \dot{x}_1(t) = x_3(t)x_2(t) - x_1(t) + h_1(t) + \Delta f_1(x) + u_1(t), \\ \dot{x}_2(t) = \epsilon_1 x_3(t) - x_3(t)x_1(t) - x_2(t) + h_2(t) + \Delta f_2(x) \\ \qquad\quad + u_2(t), \\ \dot{x}_3(t) = -\epsilon_2 x_3(t) + \epsilon_2 x_2(t) + h_3(t) + \Delta f_3(x) + u_3(t), \end{cases}$$

whereas ϵ_1, ϵ_2 represent system parameters, the definitions of the remaining symbols remain consistent with formula (23).

From reference [104], the DISZNN design formula can be described as:

$$\dot{E}(t) = -s_0^3 \int_0^t \left(\int_0^\sigma E(\tau)\mathrm{d}\tau \right)\mathrm{d}\sigma - s_0^2 \int_0^t E(\sigma)\mathrm{d}\sigma - 3s_0 E(t),$$

where s_0 represents the design parameter and the error function are the same as in formula (24).

And the controller based on DISZNN is:

$$\begin{aligned} \dot{E}(t) = &-s_0^3 \int_0^t \left(\int_0^\sigma E(\tau)\mathrm{d}\tau \right)\mathrm{d}\sigma - s_0^2 \int_0^t E(\sigma)\mathrm{d}\sigma - 3s_0 E(t) \\ &- F(X(t)) \end{aligned}$$

In the comparison of the impact of using DISZNN controller and not using DISZNN controller on PMSM Chaotic System with Uncertainties and External Disturbance, the results show that without using DISZNN controller, the state error of the system can be stabilized, but it is not zero. However, using DISZNN controller can make the state error of the system converge to zero. In order to verify the convergence performance of PMSM Chaotic System under external disturbance after using DISZNN controller, Hua used four different levels of external disturbances. The experimental results show that the controlled PMSM chaotic system designed based on DISZNN model has better external disturbance suppression ability and faster state variable convergence ability.

The synchronization of chaotic systems entails compelling a response chaotic system to track the trajectory of a master chaotic system using a constructed controller. This synchronization concept is widely applied in areas such as secure communication and information processing [105]. In 2023, Jin et al. introduced a time-varying fuzzy parameter ZNN (TVFPZNN) model aimed at facilitating the synchronization of chaotic systems in the presence of external noise [106]. A notable feature of the TVFPZNN model is its utilization of time-varying fuzzy parameters generated by fuzzy logic systems, and its effectiveness was confirmed through experimental validation.

In order to verify the outstanding performance of TVFPZNN, Jin presented two instances of synchronization involving Chen chaotic systems and autonomous chaotic systems with varying fuzzy membership functions, and subjected to three types of irregular noise.

Reference [106] demonstrates the representation of the Chen chaotic system as:

$$\begin{cases} \dot{x}_1(t) = a(x_2(t) - x_1(t)), \\ \dot{x}_2(t) = dx_1(t) - x_1(t)x_3(t) + cx_2(t), \\ \dot{x}_3(t) = x_1(t)x_2(t) - bx_3(t), \end{cases}$$

where $a = 35, b = 3, c = 12, d = 7$.

The master chaotic system affected by external noise disturbances can be represented as follows:

$$\begin{cases} \dot{x}_{m1}(t) = a(x_{m2}(t) - x_{m1}(t)) + \varpi_1(t), \\ \dot{x}_{m2}(t) = dx_{m1}(t) - x_{m1}(t)x_{m3}(t) + cx_{m2}(t) + \varpi_2(t), \\ \dot{x}_{m3}(t) = x_{m1}(t)x_{m2}(t) - bx_{m3}(t) + \varpi_3(t) \end{cases}$$

The response chaotic system with controller is described as:

$$\begin{cases} \dot{x}_{r1}(t) = a(x_{r2}(t) - x_{r1}(t)) + \mu_1(t), \\ \dot{x}_{r2}(t) = dx_{r1}(t) - x_{r1}(t)x_{r3}(t) + cx_{r2}(t) + \mu_2(t), \\ \dot{x}_{r3}(t) = x_{r1}(t)x_{r2}(t) - bx_{r3}(t) + \mu_3(t) \end{cases}$$

From reference [106], we can see that the TVFP-ZNN model is described as:

$$\begin{aligned} &f_m(x_m(t)) + \omega(t) - f_r(x_r(t)) - \mu(t) \\ &\quad = -(p^{t+2\zeta} + \alpha pt + p^2)\Psi(x_m(t) - x_r(t)) + \omega(t) \end{aligned}$$

where $x_m(t) = [x_{m1}(t), x_{m2}(t), x_{m3}(t), \ldots, x_{m3}(t)]^{\mathrm{T}}$ is the state vector of master chaotic system and $f_m(\cdot)$ is the nonlinear mapping vector function, $x_r(t) = [x_{r1}(t), x_{r2}(t), x_{r3}(t), \ldots, x_{r3}(t)]^{\mathrm{T}}$ is the state vector of response chaotic system and $f_r(\cdot)$ is the nonlinear mapping vector function, $\omega(t) = [\omega_1(t), \omega_2(t), \omega_3(t), \ldots, \omega_n(t)]^{\mathrm{T}}$ denotes the time-varying irregular external noise, $p^{t+2\zeta} +$

$\alpha pt + p^2$ is fuzzy time-varying parameter, the symbol $\Psi(\cdot)$ denotes the nonlinear SBPAF.

In Experiment B [106], a comparative evaluation of the response of the Chen chaotic system, controlled by the PT-VR-ZNN [107], AFT-ZNN [108], FPZNN [109], and TVFP-ZNN models in both noise-free and noisy environments, was conducted. The findings indicate that all four models achieve synchronization in noise-free environments, with only the TVFP-ZNN model demonstrating synchronization of the Chen chaotic system in noisy environments. The Chen chaotic system controlled by the proposed TVFP-ZNN model exhibits the fastest convergence rate and the smallest error in noise-free conditions, corroborating the exceptional performance of the TVFP-ZNN model.

In experiment C [106], synchronization of autonomous chaotic system is considered. autonomous chaotic system can be described as follows:

$$\begin{cases} \dot{x}_1(t) = p(x_2(t) - x_1(t)) + x_2(t)x_3(t), \\ \dot{x}_2(t) = (r-p)x_1(t) - x_1(t)x_3(t) + rx_2(t) \\ \dot{x}_3(t) = sx_2(t)x_2(t) - qx_3(t), \end{cases}$$

where $a = 35, b = 3, c = 12, d = 7$.

Likewise, the master chaotic system with external noise disturbance can be described as:

$$\begin{cases} \dot{x}_{m1}(t) = p(x_{m2}(t) - x_{m1}(t)) + x_{m2}(t)x_{m3}(t) + \varpi_1(t), \\ \dot{x}_{m2}(t) = (r-p)x_{m1}(t) - x_{m1}(t)x_{m3}(t) + rx_{m2}(t) + \varpi_2(t), \\ \dot{x}_{m3}(t) = sx_{m2}(t)x_{m2}(t) - qx_{m3}(t) + \varpi_3(t) \end{cases}$$

The response chaotic system with controller is described as:

$$\begin{cases} \dot{x}_{r1}(t) = p(x_{r2}(t) - x_{r1}(t)) + x_{r2}(t)x_{r3}(t) + \mu_1(t), \\ \dot{x}_{r2}(t) = (r-p)x_{r1}(t) - x_{r1}(t)x_{r3}(t) + rx_{r2}(t) + \mu_2(t), \\ \dot{x}_{r3}(t) = sx_{r2}(t)x_{r2}(t) - qx_{r3}(t) + \mu_3(t) \end{cases}$$

where $\varpi(t)$ and $\mu(t)$ represent the controllers.

The experiment compared the response of the autonomous chaotic system controlled by the PT-VR-ZNN, AFT-ZNN, FPZNN, and TVFP-ZNN models in noisy environments. The results demonstrated that the TVFP-ZNN model achieved synchronization of the Chen Chaotic System despite noise interference, with residual errors two to three orders of magnitude smaller compared to the other models. This finding reinforces the superiority of ZNN models in addressing chaotic system problems.

In 2023, Xiao et al. introduced a ZNN-based sliding mode control strategy for addressing synchronization issues in chaotic systems. The study encompassed three primary objectives: Firstly, they developed an integral sliding manifold based on zeroing neural network. Subsequently, they devised a superior controller to facilitate synchronization of chaotic systems within a predetermined timeframe. Finally, the researchers proposed a novel activation function to alleviate chattering phenomena, and experimentally validated the effectiveness of the proposed model [110].

the master chaotic system can be described as follows:

$$\begin{cases} \dot{x}_{m1}(t) = \omega_1 x_{m2}(t) + \omega_2 x_{m1}(t) - 3\omega_1 x_{m1}(t)x_{m4}^2(t), \\ \dot{x}_{m2}(t) = x_{m1}(t) - x_{m2}(t) + x_{m3}(t), \\ \dot{x}_{m3}(t) = \omega_3 x_{m2}(t) - \omega_4 x_{m3}(t), \\ \dot{x}_{m4}(t) = x_{m1}(t) \end{cases}$$

The response chaotic system with controller is described as:

$$\begin{cases} \dot{x}_{r1}(t) = \omega_1 x_{r2}(t) + \omega_2 x_{r1}(t) - 3\omega_1 x_{r1}(t)x_{r4}^2(t) + u_1(t), \\ \dot{x}_{r2}(t) = x_{r1}(t) - x_{r2}(t) + x_{r3}(t) + u_2(t), \\ \dot{x}_{r3}(t) = \omega_3 x_{r2}(t) - \omega_4 x_{r3}(t) + u_3(t), \\ \dot{x}_{r4}(t) = x_{m1}(t) + u_4(t), \end{cases}$$

where $\omega_1 = 10, \omega_2 = 2, \omega_3 = -14, \omega_4 = 0.1$.

From reference [110], the ZNN-based integral sliding manifold is designed as follows:

$$S_j(t) = E_{j\varsigma}(t) - \gamma \int_0^t F(E_{j\varsigma})(\tau)\mathrm{d}\tau,$$

where $\gamma > 0, F(\cdot)$represents a nonlinear monotonically increasing odd function.

The precise details regarding the construction of the controller can be located in the citation [110].

The experimental comparison led to the conclusion that the chaotic system, when utilizing the fixed-time sliding mode control (FTSMC) strategy, outperforms the system without it in terms of addressing the synchronization of chaotic systems. The response system employing the FTSMC strategy demonstrates superior performance in rapidly tracking the drive system's motion, leading to reduced chattering and faster convergence to zero residual errors. Additionally, it exhibits exceptional robustness when subjected to various perturbations, including constant, Gaussian, mixed harmonic, and exponential disturbances.

In 2023, Xiao et al. presented a fixed-time robust controller (FXTRC) based on ZNN [110], addressing the generalized projective synchronization of a class of chaotic systems. Additionally, they substantiated the fixed-time synchronization and robustness of FXTRC in controlling the Generalized Projective Synchronization of chaotic systems.

Xiao et al. conducted experiments on the synchronization of chaotic systems using FXTRC for three distinct chaotic systems: the Lorenz system, Lü system, and Chen system, in order to validate the superiority of ZNN-based FXTRC in addressing the synchronization of chaotic systems [110]. Due to the potential impact of different activation functions on the model's convergence performance, LAF [7], SBPAF [111], and NSBPAF [112] were employed to activate FXTRC.

The master Lorenz system can be described as:

$$\begin{cases} \dot{x}_{m1}(t) = 15(x_{m2}(t) - x_{m1}(t)) + \triangle n_1(t), \\ \dot{x}_{m2}(t) = 21x_{m1}(t) - x_{m1}(t)x_{m3}(t) + 4.8x_{m2}(t) + \triangle n_2(t), \\ \dot{x}_{m3}(t) = x_{m1}(t)x_{m2}(t) - \dfrac{41}{15}x_{m3}(t) + \triangle n_3(t), \end{cases}$$

The response system is:

$$\begin{cases} \dot{x}_{r1}(t) = 15(x_{r2}(t) - x_{r1}(t)) + u_1(t), \\ \dot{x}_{r2}(t) = 21x_{r1}(t) - x_{m1}(t)x_{r3}(t) + 4.8x_{r2}(t) + 36(x_{r1}(t) \\ \qquad -\beta x_{m1}(t)) + u_2(t), \\ \dot{x}_{m3}(t) = x_{m1}(t)x_{r2}(t) - \dfrac{41}{15}x_{r3}(t) + u_3(t), \end{cases}$$

where $\triangle_i(t)$ stands for additive noise.

The design formula is depicted as:

$$\dot{e}_i(t) = -\lambda\Psi(e_i(t)),$$

where $\Psi(\cdot)$ is a monotone increasing odd activation function.

And from the paper [110], the FXTRC can be designed as follows:

$$u_i(t) = g_i(\cdot) - \beta f_i(\cdot) + \lambda\psi(e_i(t))$$

where $f_i(\cdot)$ and $g_i(\cdot)$ refer to the functions of driver system and response system respectively.

Through comparing the error trajectories between the Lorenz master system and Lorenz response system under various initial conditions, it can be concluded that the presence of FXTRC results in error trajectories converging approximately 10 times faster than when FXTRC is not present. Furthermore, it can be further concluded that activating FXTRC using NSBPAF yields the best results.

The experimental results for the synchronization of the Lü system and Chen system align closely with those of the previous two experiments, thus they will not be reiterated here.

V. APPLICATIONS IN OTHER FIELDS

With the rapid advancement of ZNN in the last decade, its impact has been notable across various fields. Aside from its application in robotics and chaotic systems as previously mentioned, ZNN has also been utilized in image information processing [39], [113], [114], multi-dimensional spectral estimation [69], mathematical ecology [3], pendulum tracking of IPC systems [115], mobile object localization [116], [117], [118], and other areas.

In 2013, Cherif et al. introduced a novel fast online motion estimation method using the Horn and Schunck algorithm, integrating a recurrent neural network known as Discrete Zhang neural networks (DZNN) and Simoncelli's matched-pair 5-tap filters [113]. Experimental comparisons were made between this algorithm and a sequential algorithm based on the Jacobi method using synthetic and real image sequences, highlighting its accelerated convergence.

The DZNN model can be described as:

$$X_{k+1} = X_k - \tau X_k f(AX_k)/h,$$

where $\tau = \eta h > 0$ is the step size, $f(\cdot)$ denote the activation function-matrix.

In the study, Charif et al. meticulously examined the outcomes of motion field estimation using DZNN and the Jacobi method. The results from the experiments revealed that in the Yosemite image sequence, the Jacobi method displayed numerous errors after 27 iterations, with an average angular error of 8.384Â°. In contrast, our DZNN method demonstrated superior performance with an average angular error of 5.763Â° within the same number of iterations. Notably, the Jacobi method necessitated 446 iterations to achieve this precision, while the DZNN method only required 35 iterations, underscoring its faster and more consistent performance. Furthermore, validation experiments on synthetic and real images reaffirmed the speed and stability of the DZNN algorithm compared to the Jacobi method. Moreover, the DZNN method also produced satisfactory motion estimation results in the Hamburg taxi sequence. These results from the experiments provide robust evidence for the applicability of the DZNN method in practical scenarios.

In 2013, Abderrazak Benchabane and colleagues revisited the one-dimensional capon estimator in their research. They illustrated that this approach necessitates matrix inversion. Furthermore, they expanded the applicability of the method to two-dimensional and three-dimensional data sequences [69]. To achieve this, they employed discrete-Time ZNN for calculating the inverse covariance matrix of the capon spectrum, and substantiated its superiority through simulation experiments.

The simulation results cited in the scholarly literature demonstrate that the application of DZNN for covariance matrix inversion in spectral estimation has led to substantial enhancements in both accuracy and speed. Specifically, in the realm of 3D capon spectral estimation, utilizing DZNN for covariance matrix inversion has been observed to expedite convergence and yield spectral plots akin to those generated by the direct Capon method. Furthermore, when considering the intricate domain of 2D spectral estimation, the performance of the Capon method utilizing both direct and DZNN-based calculations for the correlation matrix was assessed in the context of the synthetic aperture radar (SAR) image of the MIG-25 aircraft. It was revealed that the SAR image obtained through DZNN for the matrix inversion closely resembled that derived from the direct Capon method, with significantly reduced computational time. Additionally, under the specified conditions of N=128, SNR=10dB, and M=24, the DZNN approach demonstrated notable advantages in terms of both accuracy and speed. Notably, specific simulation experiments have highlighted that the utilization of variable step sizes is a crucial factor contributing to the accelerated convergence in the online covariance matrix inversion process through DZNN. Overall, these simulation results underscore the substantial benefits of DZNN in the inversion of covariance matrices for spectral estimation, offering a more precise and expeditious solution compared to conventional methodologies.

In 2016, experts like Aleksandar Zlateski conducted a study on diverse aspects of implementing high-performance neural networks using ZNN on CPU architectures [39]. The study initially focused on parallelizing convolutional

neural networks on Intel Xeon Phi and multi-core processors, emphasizing the potential advantages of this approach in terms of training and inference performance of deep learning models. Moreover, ZNN exhibited significant outcomes in tasks such as edge detection and dendritic density computation, illustrating its extensive potential for diverse visual tasks. Additionally, an innovative task parallelization model specifically optimized for ConvNets was proposed. This model substantially enhanced training efficiency for large models by reducing memory overhead. These studies offered a comprehensive exploration of neural network computation optimization, parallel performance, and application prospects, presenting the extensive potential of ZNN when applied to CPU architectures.

In 2016, Zhang and colleagues proposed the Z-type dynamic method as a control approach to address population control challenges within the classical predator-prey Lotka-Volterra model [3]. They introduced a set of Z-type controllers for simultaneous regulation of prey and predator populations, along with individually tailored controllers for each population, and conducted theoretical analysis to ensure species preservation and ecosystem stability. The investigation highlighted the exponential convergence performance of these control laws and effectively affirmed the efficacy of all three types of Z-type control laws through corresponding simulation examples. Furthermore, the study delved into the influence of the Z-type dynamic method on population control parameter values and addressed practical application concerns.

Fronm [3], the classical predator-prey LotkaVolterra model with two exogenous measures can be described as:

$$\begin{cases} \dot{x}(t) = x(t)(\alpha - \beta y(t) - u_{prey}(t)), \\ \dot{y}(t) = y(t)(\gamma x(t) - \delta - u_{pred}(t)), \end{cases}$$

where $x(t)$ and $y(t)$ represent the populations of prey and predator species at time instant t, respectively. The positive parameters α, β, γ and δ characterize the dynamic interaction between the two species, while the functions $u_{prey}(t)$ and $u_{pred}(t)$, referred to as exogenous measures, represent the direct control variables.

The Z-type controller group, which is designed for the simultaneous control of prey and predator populations and is expressed in a closed-loop feedback format, can be described as:

$$\begin{cases} u_{prey}(t) = \dfrac{1}{x(t)}[\alpha x(t) - \beta x(t)y(t) + \lambda(x(t) - x_d(t)) \\ \qquad -\dot{x}_d(t))], \\ u_{pred}(t) = \dfrac{1}{y(t)}[\gamma x(t)y(t) - \delta y(t) + \lambda(y(t) - y_d(t)) \\ \qquad -\dot{y}_d(t))]. \end{cases}$$

In the simulation experiments, the Z-type controller group effectively regulated both predator and prey populations, causing them to exponentially converge to specified reference trajectories, thus achieving ecological balance. Additionally, the Z-type controller for indirect control of the prey population demonstrated the capability to steer the prey population towards the desired state within a short period. The Z-type controller for indirect control of the predator population also displayed effective control, ensuring the stability of the predator population. These results validate the theoretical analysis and confirm the practicality and effectiveness of Z-type controllers for population control in the Lotka-Volterra model.

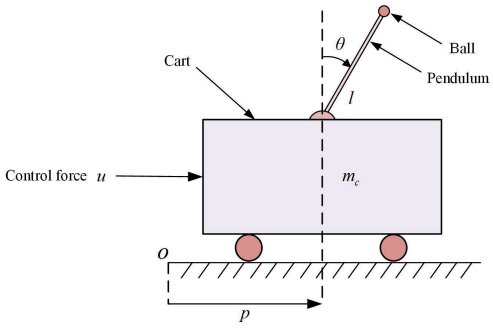

FIGURE 4. Schematic of IPC system.

In 2017, Zhang and colleagues integrated ZNN-based zeroing dynamics with conventional gradient dynamics to develop two streamlined zeroing-gradient (ZG) controllers, known as the z2g0 and z2g1 controllers, for the inverted pendulum on a cart (IPC) system [115]. The effectiveness of the ZG controllers was confirmed through simulation experiments.

The Inverted pendulum on a cart (IPC) system is inherently unstable, displaying nonlinear and underactuated characteristics. Zhang et al. investigated the control of pendulum tracking (including swinging upwards) of the IPC system's mathematical model as shown in Figure 4, where (m_c, p) denotes the mass and position of the cart, which can move freely on a horizontal plane. Additionally, m_p represents the pendulum's mass concentrated at the ball, θ is the angle between the vertical line and the pendulum (clockwise positive), l is the length of the pendulum, g is the gravitational acceleration constant, b is the viscous friction coefficient of the cart's motion, u is the control input of the IPC system, corresponding to the horizontal force applied to the cart. From [115],we can obtain the state equations of the IPC system can be expressed as:

$$\begin{cases} \dot{x}_1 = x_2, \\ \dot{x}_2 = \dfrac{u - bx_2 + m_p(lx_4^2 - g\cos x_3)\sin x_3}{m_c + m_p \sin^2 x_3}, \\ \dot{x}_3 = x_4, \\ \dot{x}_4 = \dfrac{(m_c + m_p)g\sin x_3 - (u - bx_2 + m_p l x_4^2 \sin x_3)\cos x_3}{l(m_c + m_p \sin^2 x_3)}, \end{cases}$$

where $x_1 = p, x_2 = \dot{p}, x_3 = \theta, x_4 = \dot{\theta}$ are selected as state variables.

TABLE 1. Details of the ZNN model and its application scenarios.

Model	Application Scenarios	AFs Type	Finite-time convergence	Integral structure	Discrete or Continuous	Reference
ZNN	Manipulator path tracking	Linear	No	No	Continuous	[58]
FTZNN, ITFCZNN	Manipulator path tracking	Non-linear	Yes	No	Continuous	[59], [64]
RZND	Manipulator path tracking	Linear	No	Single	Continuous	[61]
STZNN	Manipulator path tracking	Non-linear	Yes	Single	Continuous	[62]
MZNN	Manipulator path tracking	Non-linear	No	No	Continuous	[63]
T-ZNN, HADTZTM	Manipulator path tracking	linear	No	No	Discrete	[70], [72]
ED-NTZNN	Manipulator path tracking	Linear	No	Single	Discrete	[73]
VP-CDNN	Manipulator motion planning	Non-linear	No	No	Continuous	[87]
DZNN, 6SDZNN, 6SEBD-based IZNN	Manipulator motion planning	Linear	No	No	Discrete	[79], [88], [89]
FER-DZNN	Manipulator motion planning	Linear	No	Single	Discrete	[94]
NZNN	Chaotic system	Linear	No	Single	Continuous	[102]
DISZNN	Chaotic system	Linear	No	Double	Continuous	[104]
TVFP-ZNN	Chaotic system	Non-linear	Yes	No	Continuous	[106]
ZNN-based sliding mode control strategy	Chaotic system	Non-linear	No	Single	Continuous	[110]

The z2g0 controller in the form of u can be described as:

$$\begin{cases} f_1 = \ddot{y}_d + (\lambda_1 + \lambda_2)(\dot{y}_d - x_4) + \lambda_1\lambda_2(y_d - x_3), \\ f_2 = l(m_c + m_p \sin^2 x_3), \\ f_3 = (m_c + m_p)g \sin x_3, \\ f_4 = bx_2 - m_p l x_4^2 \sin x_3, \\ u = f_4 - \dfrac{f_1 f_2 - f_3}{\cos x_3}. \end{cases}$$

The z2g1controller in the form of u can be described as:

$$\begin{cases} f_1 = \ddot{y}_d + (\lambda_1 + \lambda_2)(\dot{y}_d - x_4) + \lambda_1\lambda_2(y_d - x_3), \\ f_2 = l(m_c + m_p \sin^2 x_3), \\ f_3 = (m_c + m_p)g \sin x_3, \\ f_4 = bx_2 - m_p l x_4^2 \sin x_3, \\ \dot{u} = -\gamma \cos x_3 h = -\gamma \cos x_3(\cos x_3(u - f_4) \\ \qquad +(f_1 f_2 - f_3)), \end{cases}$$

The experiment section of the article [115] demonstrated the effectiveness and superiority of the proposed z2g1 controller in addressing singularity issues, swinging up the pendulum, and tracking inverted pendulum control. Moreover, the study also confirmed the robustness of the proposed ZG controller and design method in the existence of time delays or disturbances. Additionally, the experiments illustrated the impact of relatively small values of design parameters $(\lambda_1, \lambda_2, \gamma)$ on the tracking performance of the z2g1 controller, as well as estimation of power consumption for the IPC system equipped with the z2g1 controller. Further comparative results indicated that the z2g1 controller exhibited slightly better performance than the z2g0 controller in tracking, and also maintained some characteristics of the z2g0 controller to a certain extent. Finally, theoretical analysis demonstrated the convergence performance of the z2g1 controller in control of inverted pendulum. Therefore, based on the above experimental results and comparative analysis, the proposed z2g1 controller has shown effectiveness and feasibility in overcoming singularity problems and achieving control of inverted pendulum. In 2021, Guo and colleagues proposed a zeroth-order neural network (ZNN) model to tackle the problem of dynamic matrix LQ decomposition [116]. They also demonstrated the applicability of the ZNN model by using it to localize mobile targets based on the angle of arrival (AoA) technique.

The LQ decomposition problem of dynamic matrix is described as follows:

$$A(t) = L(t)Q(t),$$

where, the matrix $A(t)$ is a representation of the smooth dynamic matrix to undergo decomposition, with $L(t)$ and $Q(t)$ denoting the lower triangular matrix and orthogonal matrix, respectively.

ZNN model is described as follows:

$$W(t)\dot{z}(t) = u(t),$$

where

$$W(t) = \begin{bmatrix} (Q^{\mathrm{T}}(t) \otimes I_n)G & I_n \otimes L(t) \\ \mathrm{zeros}(n^2, \frac{n^2+n}{2}) & (Q^{\mathrm{T}}(t) \otimes I_n)P + I_n \otimes Q^{\mathrm{T}}(t) \end{bmatrix},$$

$$z(t) = \begin{bmatrix} \mathrm{vec}(\hat{L}(t)) \\ \mathrm{vec}(Q(t)) \end{bmatrix}, u(t) = \begin{bmatrix} \mathrm{vec}(\lambda Z_1(t) + \dot{A}(t)) \\ \mathrm{vec}(\lambda Z_2(t)) \end{bmatrix},$$

Guo and colleagues effectively tackled the LQ decomposition problem for dynamic matrices using the ZNN model, proposing its application in localizing mobile objects based on the Angle of Arrival (AoA) technique. The experimental findings showcased the ZNN model's ability to produce estimated trajectories closely mirroring the actual paths during mobile object localization. Furthermore, the researchers furnished two simulation examples wherein the ZNN model was applied to address the LQ decomposition problem for dynamic matrices, serving to affirm its effectiveness and establish the reasonableness of the localization outcomes. Additionally, the experiments evidenced that the ZNN model more effectively fulfilled real-time computational requirements. These empirical findings robustly endorse the utilization of the ZNN model in the localization of mobile objects and underscore its potential practical value.

VI. CONCLUSION

The study extensively examines the application of the zeroing neural network (ZNN) model across diverse domains over the last two decades. These domains include manipulator path tracking, manipulator motion planning, chaotic systems, and others as detailed in Table 1. These applications require real-time data processing with high efficiency, and the capability of ZNN in tackling time-varying issues positions it as a frontrunner in these scenarios. The continual evolution and enhancement of the ZNN model have resulted in newly introduced ZNN variants showcasing enhanced noise immunity and faster convergence rates, thereby demonstrating exceptional performance across various disciplines. Nevertheless, numerous emerging challenges await effective resolution.

(1) How to construct a new type of nonlinear activation function to accelerate the convergence speed of the model, addressing practical application needs, especially in applications such as manipulator path tracking and motion planning.

(2) How to enhance the model's noise resistance, as it is crucial for the model's performance in practical applications

to improve its ability to resist noise and disturbances in the input data.

(3) How to expand the applicability of the ZNN model to a wider range of fields and scenarios while maintaining its efficiency and effectiveness.

Overall, this review paper provides valuable references for researchers who seek a comprehensive understanding of ZNN's applications across various domains, while also offering assistance for ZNN's future development in these fields.

REFERENCES

[1] L. Ding, L. Xiao, B. Liao, R. Lu, and H. Peng, "An improved recurrent neural network for complex-valued systems of linear equation and its application to robotic motion tracking," *Frontiers Neurorobotics*, vol. 11, p. 45, Sep. 2017.

[2] B. Liao, Z. Huang, X. Cao, and J. Li, "Adopting nonlinear activated beetle antennae search algorithm for fraud detection of public trading companies: A computational finance approach," *Mathematics*, vol. 10, no. 13, p. 2160, Jun. 2022, doi: 10.3390/math10132160.

[3] Y. Zhang, X. Yan, B. Liao, Y. Zhang, and Y. Ding, "Z-type control of populations for Lotka–Volterra model with exponential convergence," *Math. Biosci.*, vol. 272, pp. 15–23, Feb. 2016.

[4] A. Voulodimos, N. Doulamis, A. Doulamis, and E. Protopapadakis, "Deep learning for computer vision: A brief review," *Comput. Intell. Neurosci.*, vol. 2018, pp. 1–13, Feb. 2018, doi: 10.1155/2018/7068349.

[5] R. A. Jarvis, "A perspective on range finding techniques for computer vision," *IEEE Trans. Pattern Anal. Mach. Intell.*, vol. PAMI-5, no. 2, pp. 122–139, Mar. 1983.

[6] M. Benzeghiba, R. De Mori, O. Deroo, S. Dupont, T. Erbes, D. Jouvet, L. Fissore, P. Laface, A. Mertins, C. Ris, R. Rose, V. Tyagi, and C. Wellekens, "Automatic speech recognition and speech variability: A review," *Speech Commun.*, vol. 49, nos. 10–11, pp. 763–786, Oct. 2007.

[7] B. Liao and Y. Zhang, "From different ZFs to different ZNN models accelerated via Li activation functions to finite-time convergence for time-varying matrix pseudoinversion," *Neurocomputing*, vol. 133, pp. 512–522, Jun. 2014.

[8] L. Xiao, J. Dai, R. Lu, S. Li, J. Li, and S. Wang, "Design and comprehensive analysis of a noise-tolerant ZNN model with limited-time convergence for time-dependent nonlinear minimization," *IEEE Trans. Neural Netw. Learn. Syst.*, vol. 31, no. 12, pp. 5339–5348, Dec. 2020.

[9] W. Li, B. Liao, L. Xiao, and R. Lu, "A recurrent neural network with predefined-time convergence and improved noise tolerance for dynamic matrix square root finding," *Neurocomputing*, vol. 337, pp. 262–273, Apr. 2019.

[10] L. Xiao, Z. Zhang, Z. Zhang, W. Li, and S. Li, "Design, verification and robotic application of a novel recurrent neural network for computing dynamic Sylvester equation," *Neural Netw.*, vol. 105, pp. 185–196, Sep. 2018.

[11] L. Xiao, S. Li, J. Yang, and Z. Zhang, "A new recurrent neural network with noise-tolerance and finite-time convergence for dynamic quadratic minimization," *Neurocomputing*, vol. 285, pp. 125–132, Apr. 2018.

[12] L. Jin, Y. Zhang, and S. Li, "Integration-enhanced Zhang neural network for real-time-varying matrix inversion in the presence of various kinds of noises," *IEEE Trans. Neural Netw. Learn. Syst.*, vol. 27, no. 12, pp. 2615–2627, Dec. 2016.

[13] B. Liao, C. Hua, X. Cao, V. N. Katsikis, and S. Li, "Complex noise-resistant zeroing neural network for computing complex time-dependent Lyapunov equation," *Mathematics*, vol. 10, no. 15, p. 2817, Aug. 2022.

[14] X. Lv, L. Xiao, Z. Tan, and Z. Yang, "Wsbp function activated Zhang dynamic with finite-time convergence applied to Lyapunov equation," *Neurocomputing*, vol. 314, pp. 310–315, Nov. 2018.

[15] Y. Yang and Y. Zhang, "Superior robustness of power-sum activation functions in Zhang neural networks for time-varying quadratic programs perturbed with large implementation errors," *Neural Comput. Appl.*, vol. 22, no. 1, pp. 175–185, Jan. 2013.

[16] Y.-N. Zhang, Z. Li, D.-S. Guo, K. Chen, and P. Chen, "Superior robustness of using power-sigmoid activation functions in Z-type models for time-varying problems solving," in *Proc. Int. Conf. Mach. Learn. Cybern.*, vol. 2, Jul. 2013, pp. 759–764.

[17] Y. Zhang, L. Jin, and Z. Ke, "Superior performance of using hyperbolic sine activation functions in ZNN illustrated via time-varying matrix square roots finding," *Comput. Sci. Inf. Syst.*, vol. 9, no. 4, pp. 1603–1625, 2012.

[18] S. Li, S. Chen, and B. Liu, "Accelerating a recurrent neural network to finite-time convergence for solving time-varying Sylvester equation by using a sign-Bi-power activation function," *Neural Process. Lett.*, vol. 37, no. 2, pp. 189–205, Apr. 2013.

[19] J. Jin, J. Zhu, J. Gong, and W. Chen, "Novel activation functions-based ZNN models for fixed-time solving dynamirc Sylvester equation," *Neural Comput. Appl.*, vol. 34, no. 17, pp. 14297–14315, Sep. 2022.

[20] J. Dai, X. Yang, L. Xiao, L. Jia, and Y. Li, "ZNN with fuzzy adaptive activation functions and its application to time-varying linear matrix equation," *IEEE Trans. Ind. Informat.*, vol. 18, no. 4, pp. 2560–2570, Apr. 2022.

[21] B. Liao and Y. Zhang, "Different complex ZFs leading to different complex ZNN models for time-varying complex generalized inverse matrices," *IEEE Trans. Neural Netw. Learn. Syst.*, vol. 25, no. 9, pp. 1621–1631, Sep. 2014.

[22] L. Xiao, B. Liao, S. Li, and K. Chen, "Nonlinear recurrent neural networks for finite-time solution of general time-varying linear matrix equations," *Neural Netw.*, vol. 98, pp. 102–113, Feb. 2018.

[23] L. Xiao, "A new design formula exploited for accelerating Zhang neural network and its application to time-varying matrix inversion," *Theor. Comput. Sci.*, vol. 647, pp. 50–58, Sep. 2016.

[24] L. Xiao, Y. Zhang, J. Dai, K. Chen, S. Yang, W. Li, B. Liao, L. Ding, and J. Li, "A new noise-tolerant and predefined-time ZNN model for time-dependent matrix inversion," *Neural Netw.*, vol. 117, pp. 124–134, Sep. 2019.

[25] L. Xiao, Y. Zhang, K. Li, B. Liao, and Z. Tan, "A novel recurrent neural network and its finite-time solution to time-varying complex matrix inversion," *Neurocomputing*, vol. 331, pp. 483–492, Feb. 2019.

[26] L. Xiao, K. Li, Z. Tan, Z. Zhang, B. Liao, K. Chen, L. Jin, and S. Li, "Nonlinear gradient neural network for solving system of linear equations," *Inf. Process. Lett.*, vol. 142, pp. 35–40, Feb. 2019.

[27] L. Xiao and R. Lu, "Finite-time solution to nonlinear equation using recurrent neural dynamics with a specially-constructed activation function," *Neurocomputing*, vol. 151, pp. 246–251, Mar. 2015.

[28] K. Zheng, S. Li, and Y. Zhang, "Low-computational-complexity zeroing neural network model for solving systems of dynamic nonlinear equations," *IEEE Trans. Autom. Control*, early access, 2024, doi: 10.1109/TAC.2023.3319132.

[29] W. Li, L. Xiao, and B. Liao, "A finite-time convergent and noise-rejection recurrent neural network and its discretization for dynamic nonlinear equations solving," *IEEE Trans. Cybern.*, vol. 50, no. 7, pp. 3195–3207, Jul. 2020.

[30] Z. Zhang, L. Zheng, J. Weng, Y. Mao, W. Lu, and L. Xiao, "A new varying-parameter recurrent neural-network for online solution of time-varying Sylvester equation," *IEEE Trans. Cybern.*, vol. 48, no. 11, pp. 3135–3148, Nov. 2018.

[31] L. Xiao and B. Liao, "A convergence-accelerated Zhang neural network and its solution application to Lyapunov equation," *Neurocomputing*, vol. 193, pp. 213–218, Jun. 2016.

[32] L. Xiao, "A finite-time convergent neural dynamics for online solution of time-varying linear complex matrix equation," *Neurocomputing*, vol. 167, pp. 254–259, Nov. 2015.

[33] L. Xiao, "A nonlinearly activated neural dynamics and its finite-time solution to time-varying nonlinear equation," *Neurocomputing*, vol. 173, pp. 1983–1988, Jan. 2016.

[34] D. Guo, K. Li, and B. Liao, "Bi-criteria minimization with MWVN-INAM type for motion planning and control of redundant robot manipulators," *Robotica*, vol. 36, no. 5, pp. 655–675, May 2018.

[35] B. Liao and W. Liu, "Pseudoinverse-type bi-criteria minimization scheme for redundancy resolution of robot manipulators," *Robotica*, vol. 33, no. 10, pp. 2100–2113, Dec. 2015.

[36] L. Xiao, Y. Zhang, B. Liao, Z. Zhang, L. Ding, and L. Jin, "A velocity-level bi-criteria optimization scheme for coordinated path tracking of dual robot manipulators using recurrent neural network," *Frontiers Neurorobotics*, vol. 11, p. 47, Sep. 2017.

[37] L. Jin, B. Liao, M. Liu, L. Xiao, D. Guo, and X. Yan, "Different-level simultaneous minimization scheme for fault tolerance of redundant manipulator aided with discrete-time recurrent neural network," *Frontiers Neurorobotics*, vol. 11, p. 50, Sep. 2017.

[38] L. Han, Y. He, B. Liao, and C. Hua, "An accelerated double-integral ZNN with resisting linear noise for dynamic Sylvester equation solving and its application to the control of the SFM chaotic system," *Axioms*, vol. 12, no. 3, p. 287, Mar. 2023.

[39] A. Zlateski, K. Lee, and H. S. Seung, "ZNN—A fast and scalable algorithm for training 3D convolutional networks on multi-core and many-core shared memory machines," in *Proc. IEEE Int. Parallel Distrib. Process. Symp. (IPDPS)*, May 2016, pp. 801–811, doi: 10.1109/IPDPS.2016.119.

[40] Q. Xiang, B. Liao, L. Xiao, L. Lin, and S. Li, "Discrete-time noise-tolerant Zhang neural network for dynamic matrix pseudoinversion," *Soft Comput.*, vol. 23, no. 3, pp. 755–766, Feb. 2019.

[41] L. Xiao, K. Li, and M. Duan, "Computing time-varying quadratic optimization with finite-time convergence and noise tolerance: A unified framework for zeroing neural network," *IEEE Trans. Neural Netw. Learn. Syst.*, vol. 30, no. 11, pp. 3360–3369, Nov. 2019.

[42] Z. Zhang, L. Zheng, L. Li, X. Deng, L. Xiao, and G. Huang, "A new finite-time varying-parameter convergent-differential neural-network for solving nonlinear and nonconvex optimization problems," *Neurocomputing*, vol. 319, pp. 74–83, Nov. 2018.

[43] X. Lv, L. Xiao, and Z. Tan, "Improved Zhang neural network with finite-time convergence for time-varying linear system of equations solving," *Inf. Process. Lett.*, vol. 147, pp. 88–93, Jul. 2019.

[44] L. Xiao, Q. Yi, J. Dai, K. Li, and Z. Hu, "Design and analysis of new complex zeroing neural network for a set of dynamic complex linear equations," *Neurocomputing*, vol. 363, pp. 171–181, Oct. 2019.

[45] L. Xiao, H. Tan, L. Jia, J. Dai, and Y. Zhang, "New error function designs for finite-time ZNN models with application to dynamic matrix inversion," *Neurocomputing*, vol. 402, pp. 395–408, Aug. 2020.

[46] L. Xiao, S. Li, K. Li, L. Jin, and B. Liao, "Co-design of finite-time convergence and noise suppression: A unified neural model for time varying linear equations with robotic applications," *IEEE Trans. Syst., Man, Cybern., Syst.*, vol. 50, no. 12, pp. 5233–5243, Dec. 2020.

[47] Z. Li, B. Liao, F. Xu, and D. Guo, "A new repetitive motion planning scheme with noise suppression capability for redundant robot manipulators," *IEEE Trans. Syst., Man, Cybern., Syst.*, vol. 50, no. 12, pp. 5244–5254, Dec. 2020.

[48] Y. Zhang, S. Li, S. Kadry, and B. Liao, "Recurrent neural network for kinematic control of redundant manipulators with periodic input disturbance and physical constraints," *IEEE Trans. Cybern.*, vol. 49, no. 12, pp. 4194–4205, Dec. 2019.

[49] C. Hua, X. Cao, Q. Xu, B. Liao, and S. Li, "Dynamic neural network models for time-varying problem solving: A survey on model structures," *IEEE Access*, vol. 11, pp. 65991–66008, 2023.

[50] L. Jin, S. Li, B. Liao, and Z. Zhang, "Zeroing neural networks: A survey," *Neurocomputing*, vol. 267, pp. 597–604, Dec. 2017.

[51] W. Ye, Z. Li, C. Yang, J. Sun, C.-Y. Su, and R. Lu, "Vision-based human tracking control of a wheeled inverted pendulum robot," *IEEE Trans. Cybern.*, vol. 46, no. 11, pp. 2423–2434, Nov. 2016.

[52] G. Hu, N. Gans, N. Fitz-Coy, and W. Dixon, "Adaptive homography-based visual servo tracking control via a quaternion formulation," *IEEE Trans. Control Syst. Technol.*, vol. 18, no. 1, pp. 128–135, Jan. 2010.

[53] O. Linda and M. Manic, "Self-organizing fuzzy haptic teleoperation of mobile robot using sparse sonar data," *IEEE Trans. Ind. Electron.*, vol. 58, no. 8, pp. 3187–3195, Aug. 2011.

[54] L. Li, S. Yan, X. Yu, Y. K. Tan, and H. Li, "Robust multiperson detection and tracking for mobile service and social robots," *IEEE Trans. Syst., Man, Cybern. B, Cybern.*, vol. 42, no. 5, pp. 1398–1412, Oct. 2012.

[55] L. Xiao and Y. Zhang, "A new performance index for the repetitive motion of mobile manipulators," *IEEE Trans. Cybern.*, vol. 44, no. 2, pp. 280–292, Feb. 2014.

[56] L. Jin, S. Li, X. Luo, Y. Li, and B. Qin, "Neural dynamics for cooperative control of redundant robot manipulators," *IEEE Trans. Ind. Informat.*, vol. 14, no. 9, pp. 3812–3821, Sep. 2018.

[57] R. G. Roberts and A. A. Maciejewski, "Repeatable generalized inverse control strategies for kinematically redundant manipulators," *IEEE Trans. Autom. Control*, vol. 38, no. 5, pp. 689–699, May 1993.

[58] K. Tchon and R. Muszynski, "Singular inverse kinematic problem for robotic manipulators: A normal form approach," *IEEE Trans. Robot. Autom.*, vol. 14, no. 1, pp. 93–104, Feb. 1998.

[59] L. Xiao and Y. Zhang, "Solving time-varying inverse kinematics problem of wheeled mobile manipulators using Zhang neural network with exponential convergence," *Nonlinear Dyn.*, vol. 76, no. 2, pp. 1543–1559, Apr. 2014.

[60] L. Xiao, B. Liao, S. Li, Z. Zhang, L. Ding, and L. Jin, "Design and analysis of FTZNN applied to the real-time solution of a nonstationary Lyapunov equation and tracking control of a wheeled mobile manipulator," *IEEE Trans. Ind. Informat.*, vol. 14, no. 1, pp. 98–105, Jan. 2018.

[61] Ş. Yildirim and Í. Eski, "Noise analysis of robot manipulator using neural networks," *Robot. Comput.-Integr. Manuf.*, vol. 26, no. 4, pp. 282–290, Aug. 2010.

[62] D. Chen and Y. Zhang, "Robust zeroing neural-dynamics and its time-varying disturbances suppression model applied to mobile robot manipulators," *IEEE Trans. Neural Netw. Learn. Syst.*, vol. 29, no. 9, pp. 4385–4397, Sep. 2018.

[63] D. Chen, S. Li, and Q. Wu, "A novel supertwisting zeroing neural network with application to mobile robot manipulators," *IEEE Trans. Neural Netw. Learn. Syst.*, vol. 32, no. 4, pp. 1776–1787, Apr. 2021.

[64] Y. Zhang and J. Wang, "Recurrent neural networks for nonlinear output regulation," *Automatica*, vol. 37, no. 8, pp. 1161–1173, Aug. 2001.

[65] J. Jin and J. Gong, "An interference-tolerant fast convergence zeroing neural network for dynamic matrix inversion and its application to mobile manipulator path tracking," *Alexandria Eng. J.*, vol. 60, no. 1, pp. 659–669, Feb. 2021.

[66] D. Chen, X. Cao, and S. Li, "A multi-constrained zeroing neural network for time-dependent nonlinear optimization with application to mobile robot tracking control," *Neurocomputing*, vol. 460, pp. 331–344, Oct. 2021.

[67] J. Luo, H. Yang, L. Yuan, H. Chen, and X. Wang, "Hyperbolic tangent variant-parameter robust ZNN schemes for solving time-varying control equations and tracking of mobile robot," *Neurocomputing*, vol. 510, pp. 218–232, Oct. 2022.

[68] X. Lan, J. Jin, and H. Liu, "Towards non-linearly activated ZNN model for constrained manipulator trajectory tracking," *Frontiers Phys.*, vol. 11, Mar. 2023, Art. no. 1159212.

[69] A. Benchabane, A. Bennia, F. Charif, and A. Taleb-Ahmed, "Multi-dimensional capon spectral estimation using discrete Zhang neural networks," *Multidimensional Syst. Signal Process.*, vol. 24, no. 3, pp. 583–598, Sep. 2013.

[70] Y. Zhang, Y. Zhang, D. Chen, Z. Xiao, and X. Yan, "From Davidenko method to Zhang dynamics for nonlinear equation systems solving," *IEEE Trans. Syst., Man, Cybern., Syst.*, vol. 47, no. 11, pp. 2817–2830, Nov. 2017.

[71] L. Jin and Y. Zhang, "Discrete-time Zhang neural network of $O(\tau^3)$ pattern for time-varying matrix pseudoinversion with application to manipulator motion generation," *Neurocomputing*, vol. 142, pp. 165–173, Oct. 2014.

[72] B. Liao, Y. Zhang, and L. Jin, "Taylor $O(h^3)$ discretization of ZNN models for dynamic equality-constrained quadratic programming with application to manipulators," *IEEE Trans. Neural Netw. Learn. Syst.*, vol. 27, no. 2, pp. 225–237, Feb. 2016.

[73] Z. Sun, Y. Liu, L. Wei, K. Liu, L. Jin, and L. Ren, "Two DTZNN models of $O(\tau^4)$ pattern for online solving dynamic system of linear equations: Application to manipulator motion generation," *IEEE Access*, vol. 8, pp. 36624–36638, 2020.

[74] K. Liu, Y. Liu, Y. Zhang, L. Wei, Z. Sun, and L. Jin, "Five-step discrete-time noise-tolerant zeroing neural network model for time-varying matrix inversion with application to manipulator motion generation," *Eng. Appl. Artif. Intell.*, vol. 103, Aug. 2021, Art. no. 104306.

[75] W. Wu and Y. Zhang, "Discrete gradient-zeroing neural dynamics for future Moore–Penrose inverse with application to tracking control of manipulator," *Expert Syst. Appl.*, vol. 227, Oct. 2023, Art. no. 120249.

[76] J. Chen, J. Guo, and Y. Zhang, "General ten-instant DTDMSR model for dynamic matrix square root finding," *Cybern. Syst.*, vol. 52, no. 1, pp. 127–143, Jan. 2021.

[77] D. Chen, S. Li, Q. Wu, and X. Luo, "Super-twisting ZNN for coordinated motion control of multiple robot manipulators with external disturbances suppression," *Neurocomputing*, vol. 371, pp. 78–90, Jan. 2020.

[78] A. H. Khan, S. Li, and X. Luo, "Obstacle avoidance and tracking control of redundant robotic manipulator: An RNN-based metaheuristic approach," *IEEE Trans. Ind. Informat.*, vol. 16, no. 7, pp. 4670–4680, Jul. 2020.

[79] H. Lu, L. Jin, J. Zhang, Z. Sun, S. Li, and Z. Zhang, "New joint-drift-free scheme aided with projected ZNN for motion generation of redundant robot manipulators perturbed by disturbances," *IEEE Trans. Syst., Man, Cybern., Syst.*, vol. 51, no. 9, pp. 5639–5651, Sep. 2021.

[80] B. Qiu, J. Guo, S. Yang, P. Yu, and N. Tan, "A novel discretized ZNN model for velocity layer weighted multicriteria optimization of robotic manipulators with multiple constraints," *IEEE Trans. Ind. Informat.*, vol. 19, no. 5, pp. 6717–6728, May 2023.

[81] L. Jin, J. Zhang, X. Luo, M. Liu, S. Li, L. Xiao, and Z. Yang, "Perturbed manipulability optimization in a distributed network of redundant robots," *IEEE Trans. Ind. Electron.*, vol. 68, no. 8, pp. 7209–7220, Aug. 2021.
[82] L. Jin and S. Li, "Distributed task allocation of multiple robots: A control perspective," *IEEE Trans. Syst., Man, Cybern., Syst.*, vol. 48, no. 5, pp. 693–701, May 2018.
[83] A. M. Zanchettin, L. Bascetta, and P. Rocco, "Achieving humanlike motion: Resolving redundancy for anthropomorphic industrial manipulators," *IEEE Robot. Autom. Mag.*, vol. 20, no. 4, pp. 131–138, Dec. 2013.
[84] L. Jin, Y. Zhang, S. Li, and Y. Zhang, "Modified ZNN for time-varying quadratic programming with inherent tolerance to noises and its application to kinematic redundancy resolution of robot manipulators," *IEEE Trans. Ind. Electron.*, vol. 63, no. 11, pp. 6978–6988, Nov. 2016.
[85] F.-T. Cheng, T.-H. Chen, and Y.-Y. Sun, "Resolving manipulator redundancy under inequality constraints," *IEEE Trans. Robot. Autom.*, vol. 10, no. 1, pp. 65–71, Feb. 1989.
[86] F.-T. Cheng, R.-J. Sheu, and T.-H. Chen, "The improved compact QP method for resolving manipulator redundancy," *IEEE Trans. Syst., Man, Cybern.*, vol. 25, no. 11, pp. 1521–1530, 1995.
[87] Z. Zhang, T. Fu, Z. Yan, L. Jin, L. Xiao, Y. Sun, Z. Yu, and Y. Li, "A varying-parameter convergent-differential neural network for solving joint-angular-drift problems of redundant robot manipulators," *IEEE/ASME Trans. Mechatronics*, vol. 23, no. 2, pp. 679–689, Apr. 2018.
[88] M. Yang, Y. Zhang, N. Tan, and H. Hu, "Concise discrete ZNN controllers for end-effector tracking and obstacle avoidance of redundant manipulators," *IEEE Trans. Ind. Informat.*, vol. 18, no. 5, pp. 3193–3202, May 2022.
[89] M. Yang, Y. Zhang, Z. Zhang, and H. Hu, "6-step discrete ZNN model for repetitive motion control of redundant manipulator," *IEEE Trans. Syst., Man, Cybern., Syst.*, vol. 52, no. 8, pp. 4969–4980, Aug. 2022.
[90] D. Guo, Z. Li, A. H. Khan, Q. Feng, and J. Cai, "Repetitive motion planning of robotic manipulators with guaranteed precision," *IEEE Trans. Ind. Informat.*, vol. 17, no. 1, pp. 356–366, Jan. 2021.
[91] M. Liu, L. He, and M. Shang, "Dynamic neural network for bicriteria weighted control of robot manipulators," *IEEE Trans. Neural Netw. Learn. Syst.*, vol. 34, no. 8, pp. 4570–4583, Aug. 2023.
[92] Z. Zhang, L. Zheng, J. Yu, Y. Li, and Z. Yu, "Three recurrent neural networks and three numerical methods for solving a repetitive motion planning scheme of redundant robot manipulators," *IEEE/ASME Trans. Mechatronics*, vol. 22, no. 3, pp. 1423–1434, Jun. 2017.
[93] N. Tan, P. Yu, M. Zhang, and C. Li, "Toward unified adaptive teleoperation based on damping ZNN for robot manipulators with unknown kinematics," *IEEE Trans. Ind. Electron.*, vol. 70, no. 9, pp. 9227–9236, Sep. 2023.
[94] B. Qiu, J. Guo, M. Mao, and N. Tan, "A fuzzy-enhanced robust DZNN model for future multiconstrained nonlinear optimization with robotic manipulator control," *IEEE Trans. Fuzzy Syst.*, vol. 32, no. 1, pp. 160–173, Jan. 2024.
[95] E. N. Lorenz, "Deterministic nonperiodic flow," *J. Atmos. Sci.*, vol. 20, no. 2, pp. 130–141, Mar. 1963.
[96] M. Tuna and C. B. Fidan, "Electronic circuit design, implementation and FPGA-based realization of a new 3D chaotic system with single equilibrium point," *Optik*, vol. 127, no. 24, pp. 11786–11799, Dec. 2016.
[97] H. Yu, G. Cai, and Y. Li, "Dynamic analysis and control of a new hyperchaotic finance system," *Nonlinear Dyn.*, vol. 67, no. 3, pp. 2171–2182, Feb. 2012.
[98] J. Brindley, T. Kapitaniak, and L. Kocarev, "Controlling chaos by chaos in geophysical systems," *Geophys. Res. Lett.*, vol. 22, no. 10, pp. 1257–1260, May 1995.
[99] B. Naderi and H. Kheiri, "Exponential synchronization of chaotic system and application in secure communication," *Optik*, vol. 127, no. 5, pp. 2407–2412, Mar. 2016.
[100] W. He, T. Luo, Y. Tang, W. Du, Y.-C. Tian, and F. Qian, "Secure communication based on quantized synchronization of chaotic neural networks under an event-triggered strategy," *IEEE Trans. Neural Netw. Learn. Syst.*, vol. 31, no. 9, pp. 3334–3345, Sep. 2020.
[101] M. Rasouli, A. Zare, M. Hallaji, and R. Alizadehsani, "The synchronization of a class of time-delayed chaotic systems using sliding mode control based on a fractional-order nonlinear PID sliding surface and its application in secure communication," *Axioms*, vol. 11, no. 12, p. 738, Dec. 2022.
[102] S. B. Aoun, N. Derbel, H. Jerbi, T. E. Simos, S. D. Mourtas, and V. N. Katsikis, "A quaternion Sylvester equation solver through noise-resilient zeroing neural networks with application to control the SFM chaotic system," *AIMS Math.*, vol. 8, no. 11, pp. 27376–27395, 2023.
[103] J. Sun, X. Zhao, J. Fang, and Y. Wang, "Autonomous memristor chaotic systems of infinite chaotic attractors and circuitry realization," *Nonlinear Dyn.*, vol. 94, no. 4, pp. 2879–2887, Dec. 2018.
[104] C. Hua, X. Cao, S. Li, and B. Liao, "Dual-integral structure zeroing neural network for computing dynamic complex matrix inverse with application to chaotic control," *SSRN J.*, Sep. 2023, doi: 10.2139/ssrn.4365528.
[105] Q. Zhang, J. Lu, J. Lu, and C. K. Tse, "Adaptive feedback synchronization of a general complex dynamical network with delayed nodes," *IEEE Trans. Circuits Syst. II, Exp. Briefs*, vol. 55, no. 2, pp. 183–187, Feb. 2008.
[106] J. Jin, W. Chen, A. Ouyang, F. Yu, and H. Liu, "A time-varying fuzzy parameter zeroing neural network for the synchronization of chaotic systems," *IEEE Trans. Emerg. Topics Comput. Intell.*, vol. 8, no. 1, pp. 364–376, Feb. 2023, doi: 10.1109/TETCI.2023.3301793.
[107] L. A. Zadeh, "Fuzzy sets," *Inf. Control*, vol. 8, no. 3, pp. 338–353, 1965.
[108] L. Jia, L. Xiao, J. Dai, and Y. Cao, "A novel fuzzy-power zeroing neural network model for time-variant matrix Moore–Penrose inversion with guaranteed performance," *IEEE Trans. Fuzzy Syst.*, vol. 29, no. 9, pp. 2603–2611, Sep. 2021.
[109] F. Yu, Z. Zhang, H. Shen, Y. Huang, S. Cai, and S. Du, "FPGA implementation and image encryption application of a new PRNG based on a memristive Hopfield neural network with a special activation gradient," *Chin. Phys. B*, vol. 31, no. 2, Jan. 2022, Art. no. 020505.
[110] L. Xiao, L. Li, P. Cao, and Y. He, "A fixed-time robust controller based on zeroing neural network for generalized projective synchronization of chaotic systems," *Chaos, Solitons Fractals*, vol. 169, Apr. 2023, Art. no. 113279.
[111] L. Han, B. Liao, Y. He, and X. Xiao, "Dual noise-suppressed ZNN with predefined-time convergence and its application in matrix inversion," in *Proc. 11th Int. Conf. Intell. Control Inf. Process. (ICICIP)*, Dec. 2021, pp. 410–415, doi: 10.1109/ICICIP53388.2021.9642164.
[112] J. Dai, L. Jia, and L. Xiao, "Design and analysis of two prescribed-time and robust ZNN models with application to time-variant stein matrix equation," *IEEE Trans. Neural Netw. Learn. Syst.*, vol. 32, no. 4, pp. 1668–1677, Apr. 2021.
[113] F. Charif, A. Benchabane, N. Djedi, and A. Taleb-Ahmed, "Horn & schunck meets a discrete Zhang neural networks for computing 2D optical flow," in *Proc. Int. Conf. Electron.*, 2013.
[114] L. Xiao, X. Li, P. Cao, Y. He, W. Tang, J. Li, and Y. Wang, "A dynamic-varying parameter enhanced ZNN model for solving time-varying complex-valued tensor inversion with its application to image encryption," *IEEE Trans. Neural Netw. Learn. Syst.*, early access, 2023, doi: 10.1109/TNNLS.2023.3270563.
[115] Y. Zhang, B. Qiu, B. Liao, and Z. Yang, "Control of pendulum tracking (including swinging up) of IPC system using zeroing-gradient method," *Nonlinear Dyn.*, vol. 89, no. 1, pp. 1–25, Jul. 2017.
[116] J. Guo, B. Qiu, M. Yang, and Y. Zhang, "Zhang neural network model for solving LQ decomposition problem of dynamic matrix with application to mobile object localization," in *Proc. Int. Joint Conf. Neural Netw. (IJCNN)*, Jul. 2021, pp. 1–6, doi: 10.1109/IJCNN52387.2021.9533326.
[117] L. Xiao, Y. He, Y. Li, and J. Dai, "Design and analysis of two nonlinear ZNN models for matrix LR and QR factorization with application to 3D moving target location," *IEEE Trans. Ind. Informat.*, vol. 19, no. 6, pp. 7424–7434, Jun. 2023.
[118] Y. He, L. Xiao, F. Sun, and Y. Wang, "A variable-parameter ZNN with predefined-time convergence for dynamic complex-valued Lyapunov equation and its application to AOA positioning," *Appl. Soft Comput.*, vol. 130, Nov. 2022, Art. no. 109703.

TINGLEI WANG received the B.S. degree in electronic and information engineering from Jishou University, Jishou, China, in 2023, where he is currently pursuing the master's degree in electronic information with the College of Computer Science and Engineering.

His research interests include dynamic neural networks, robotics, and multi-agent systems.

ZHEN ZHANG received the Ph.D. degree in electronic science and technology from Northwestern Polytechnical University, Changsha, China, in 2020.

He is currently an Associate Professor in electronic information engineering with Changsha University. He has published over ten articles in various journals/conferences. His current interests include the research of neural network, signal processing, and pattern recognition. His research interests include dynamic neural networks, robotics, and multi-agent systems.

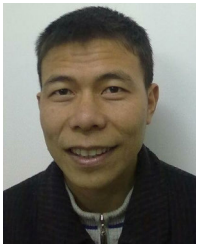

YUN HUANG received the Ph.D. degree in computer software and theory from Sun Yat-sen University, Guangzhou, China, in 2017. He is currently an Associate Professor with the College of Computer Science and Engineering, Jishou University. He has published over 20 articles in various journals/conferences. His current research interests include neural networks and graph processing. His research interests include dynamic neural networks, robotics, and multi-agent systems.

BOLIN LIAO received the Ph.D. degree in communication and information systems from Sun Yat-sen University, Guangzhou, China, in 2015. He is currently a Professor with the College of Computer Science and Engineering, Jishou University. He has published over 70 articles in various journals/conferences. His current research interests include neural networks, robotics, and nonlinear control.

SHUAI LI (Senior Member, IEEE) received the B.E. degree in precision mechanical engineering from Hefei University of Technology, China, in 2005, the M.E. degree in automatic control engineering from the University of Science and Technology of China, China, in 2008, and the Ph.D. degree in electrical and computer engineering from the Stevens Institute of Technology, Hoboken, NJ, USA, in 2014. He is currently a Full Professor with the Faculty of Information Technology and Electrical Engineering, University of Oulu, Finland. He is also an Adjunct Professor with the Technology Research Center of Finland (VTT). His current research interests include robotics, autonomous manufacturing, dynamic neural networks, machine learning, and autonomous systems.